A Thesis for the Degree of Doctor of Philosophy

Functional and Regulatory Characteristics of *Vibrio vulnificus* Alkyl Hydroperoxide Reductase (AhpC1) and Catalase (KatG)

패혈증 비브리오균의 항산화효소 alkyl hydroperoxide reductase와 catalase의 기능특성과 조절기전 연구

August, 2013

Lee, Hyun Sung

Department of Agricultural Biotechnology

College of Agriculture and Life Science

Seoul National University

Abstract

Lee, Hyun Sung

Department of Agricultural Biotechnology

The Graduate School

Seoul National University

Pathogens have evolved sophisticated mechanisms to survive oxidative stresses imposed by host defense systems, and the mechanisms are closely linked to their virulence. In the present study, *ahpC*1 and *katG*, homologues of *E. coli ahpC* encoding a peroxiredoxin and *katG* encoding a bifunctional catalase-peroxidase, respectively, were identified among the *Vibrio vulnificus* genes specifically induced by exposure to H_2O_2. The *ahpC*1 mutant was susceptible to various oxidative stress induced by H_2O_2, *tert*-butyl hydroperoxide (*t*-BOOH), and cumene hydroperoxide (CHP). In contrast, the *katG* mutant was more sensitive to H_2O_2 than the *ahpC*1 mutant and was not sensitive to oxidative stress induced by *t*-BOOH and CHP. The purified AhpC1 reduced H_2O_2 and *t*-BOOH in the presence of AhpF and NADH as a hydrogen donor. It revealed that *V. vulnificus* AhpC1 is a NADH-dependent

peroxiredoxin and constitutes a peroxide reductase system with AhpF. In addition, the catalase activity of KatG was determined using native polyacrylamide gel electrophoresis, indicating that *V. vulnificus* KatG has an antioxidant function against H_2O_2. Compared to wild type, the *ahpC*1 and *katG* mutants exhibited less cytotoxicity toward INT-407 epithelial cells *in vitro* and reduced virulence in a mouse model. To define the promoters of *ahpC*1 and *katG*, P_{ahpC1} and P_{katG}, primer extensions were performed, showing that the transcriptional start sites of *ahpC*1 and *katG* were determined and putative -10 and -35 regions of the promoters were predicted. In addition, there were OxyR binding consensus sequences located in the upstream of -35 regions of P_{ahpC1} and P_{katG}. In order to verify whether the redox sensing transcriptional regulator, OxyR, regulates the expression levels of *ahpC*1 and *katG* in *V. vulnificus*, qRT-PCR was performed using the RNA derived from wild type and the *oxyR* mutant treated with H_2O_2. The results showed that the expression levels of both *ahpC*1 and *katG* in the *oxyR* mutant were significantly reduced as compared to those in the wild type. It indicated that the expression of *ahpC*1 and *katG* is positive regulated by OxyR under oxidative stress. Both gel mobility shift assay and DNase I footprinting experiment using either oxidized or reduced OxyR revealed that the two forms of OxyR binds to the OxyR binding consensus sequences

located in the P_{ahpC1} and P_{katG}. Interestingly, reduced OxyR bound to the -35 region of P_{ahpC1} and -10 region of P_{katG}, indicating that the reduced OxyR may block RNA polymerase binding to the P_{ahpC1} and P_{katG}. In order to confirm that the expression of *ahpC*1 and *katG* was repressed by reduced OxyR, C199S-OxyR mutant, mimicking reduced OxyR, was constructed and then qRT-PCR was performed using the RNA isolated from wild type and C199S-OxyR mutant treated with H_2O_2. Compared to the expression levels of *ahpC*1 and *katG* in wild type, those in C199S-OxyR mutant were significantly reduced, indicating that reduced OxyR repressed the expression of *ahpC*1 and *katG*. In some bacteria, it has been known that *ahpC* and *ahpF* are an operon. In order to confirm whether the *V. vulnificus ahpC*1 and *ahpF* genes are an operon, northern blot analysis was performed, indicating that transcription of *ahpC*1*F* results in two different transcripts, *ahpC*1 transcript and *ahpC*1*F* transcript. Mutational analysis of the regulatory region suggested that the *ahpC*1*F* operon has a single promoter, P_{ahpC1}. These results indicated that the *ahpC*1 transcript results from attenuation of the *ahpC*1*F* transcript at the *ahpC*1 and *ahpF* intergenic region. The 3'end of *ahpC*1 transcript was determined by 3'RACE and a potential stem-loop structure responsible for the transcriptional attenuation was predicted in the *ahpC*1 and *ahpF* intergenic region. To confirm whether the transcription of

*ahpC*1*F* can be attenuated by the stem-loop structure, a reporter containing the P_{ahpC1} fused to promoterless *lux* genes was constructed. Several DNA fragments of the *ahpC*1 and *ahpF* intergenic region were inserted downstream of P_{ahpC1}, and only the DNA fragment containing the predicted stem-loop structure had the reporter RLU reduced. These results indicated that the *ahpC*1*F* operon is regulated by a single promoter and the *ahpC*1 and *ahpF* intergenic region attenuator.

Key words: *Vibrio vulnificus*, AhpC1, KatG, oxidative stress, OxyR, AhpF

Student Number: 2007-23171

Contents

List of Tables

List of Figures

Chapter I.

Introduction

I-1. *Vibrio vulnificus*

Vibrio vulnificus, belongs to *Vibrio* genus in *Vibrionaceae*, is a species of Gram-negative, curved, and rod-shaped bacteria with a single flagellum. This bacterium is found in estuarine and coastal marine environments worldwide and frequently contaminates oyster and other seafood (Hoi *et al*., 1998; Myatt and Davis, 1989). This pathogenic marine bacterium is the causative agent of food-borne diseases such as life-threatening septicemia and possibly gastroenteritis in individuals with underlying predisposing conditions (Linkous and Oliver, 1999; Strom and Paranjpye, 2000; Jones and Oliver, 2009). The characteristic symptoms of these diseases include fever, chills, nausea, hypotensive septic shock, and the formation of secondary lesions on the extremities of patients (Jones and Oliver, 2009). The latent period for septicemia is approximately 10 days in length, the time from infection until individual becomes infectious (Feldhusen, 2000). The mortality rate from septicemia is exceeding 50% and death can occur within one to two days after the first signs of illness (Linkous and Oliver, 1999; Jones and Oliver, 2009). Interestingly, most of the death cases of septicemia caused by *V. vulnificus* were male. Although it has been not been reported the exact mechanism for the gender association, it has been suggested that the

estrogen, a major female hormone, is involved. Estrogen would protect the effect of LPS endotoxin which is responsible for potentially fatal hypotension of infection (Merkel *et al*., 2001).

I-2. Oxidative stress

Oxidative stress caused by increased levels of reactive oxygen species (ROS) such as superoxide anion ($O2^-$), hydrogen peroxide (H_2O_2), and hydroxyl radical ($^{\cdot}OH$) can lead to the damage of all cellular components including protein, DNA and membrane lipid. Although incomplete reduction of oxygen during respiration and aerobic metabolism is the main source of endogenous ROS for bacterial cells, exposure to metals and redox-active chemicals also cause increased levels of the ROS (Storz and Zheng, 2000). In addition, pathogenic bacteria are inevitably exposed to ROS that are crucial to host defense for the optimal microcidal activity of neutrophils and other phagocytes (Miller and Britigan, 1997). Therefore, pathogens have evolved sophisticated mechanisms to survive oxidative stresses imposed by not only enodogenous sources but also host defense systems, and the mechanisms are closely linked to their virulence (Storz and Zheng, 2000).

I-3. The object of this study

The Centers for Disease Control estimates that approximately 94 persons in the United States are infected with *V. vulnificus*, resulting in 37 deaths per year (Mead PS *et al*., 1999). Therefore, it is important to eliminate *V. vulnificus* existed in raw oyster and other seafood. In addition, it is also necessary to prevent contamination with *V. vulnificus* caused by cross-contamination during transport or pre-treatment processing in food industry. There are many methods for sterilization, and the utilization of oxidative stress induced by H_2O_2, chlorine, and chlorine dioxide generally used in food industry is the one among these methods. However the concentration of sanitizer used in food industry is limited because the quality of foods can be diminished. In addition, because *V. vulnificus* has a defense mechanism against oxidative stress, it can be survival during sterilization processing. Therefore, if the genes associated with oxidative stress response were identified and then regulated, the survival of *V. vulnificus* could be sufficiently controlled under oxidative stress induced by low concentration of sanitizer which does not reduce the quality of foods. In present study, to find the genes associated with oxidative stress response, microarray was performed using the RNA isolated from *V. vulnificus* treated with or without

H_2O_2, indicating that the expression levels of about 200 genes from various category of group (COG) were changed (Fig. I-1). Among these genes, some were selected and then confirmed by qRT-PCR. Through these results, *ahpC*1 (GenBank accession number VVMO6_03966, www.ncbi.nlm.nih.gov) and *katG* (GenBank accession number VVMO6_01712) genes were identified as candidates for further study because their expression levels were increased under H_2O_2 and the ratios of increase were high (Fig. I-2). This study intends to acquire further knowledge of the functional roles and regulation of *V. vulnificus ahpC*1 and *katG* under oxidative stress.

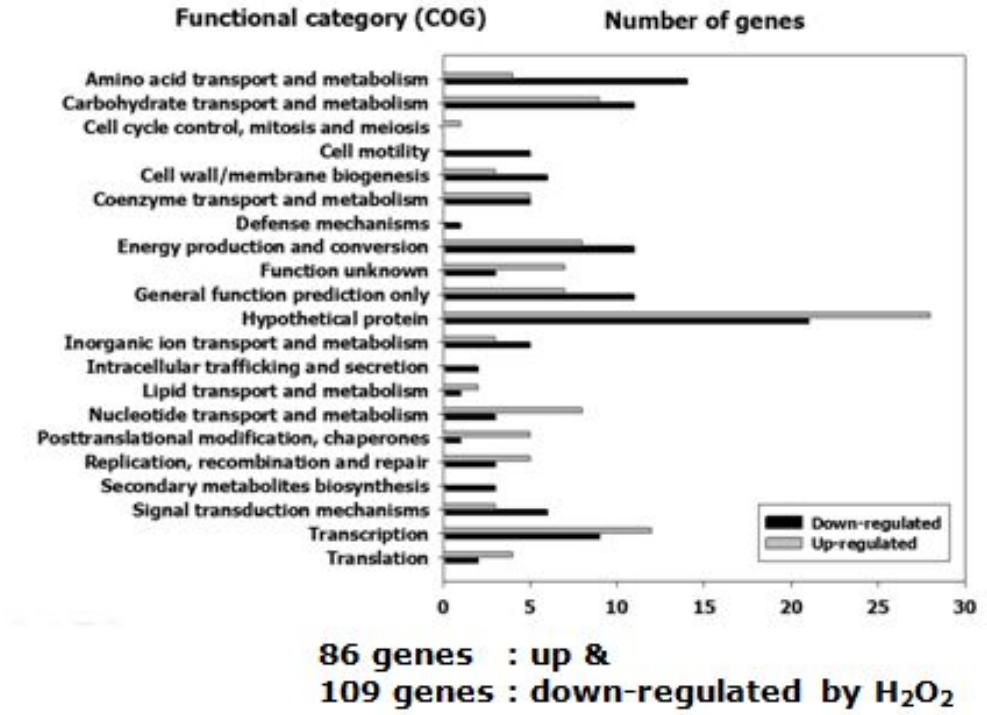

Figure I- 1. Number of genes induced by H_2O_2

Genes with expression ratios of ≥ 2 on the basis of microarray analysis were considered as being regulated under H_2O_2. Functional categories (COG) containing at least one gene are presented and based on the database of the *V. vulnificus* MO6-24/O genome (Park *et al*., 2011) which are retrieved from GenBank (CP002469; CP002470). Gray and black bars represent the genes up-regulated and down-regulated under H_2O_2, respectively.

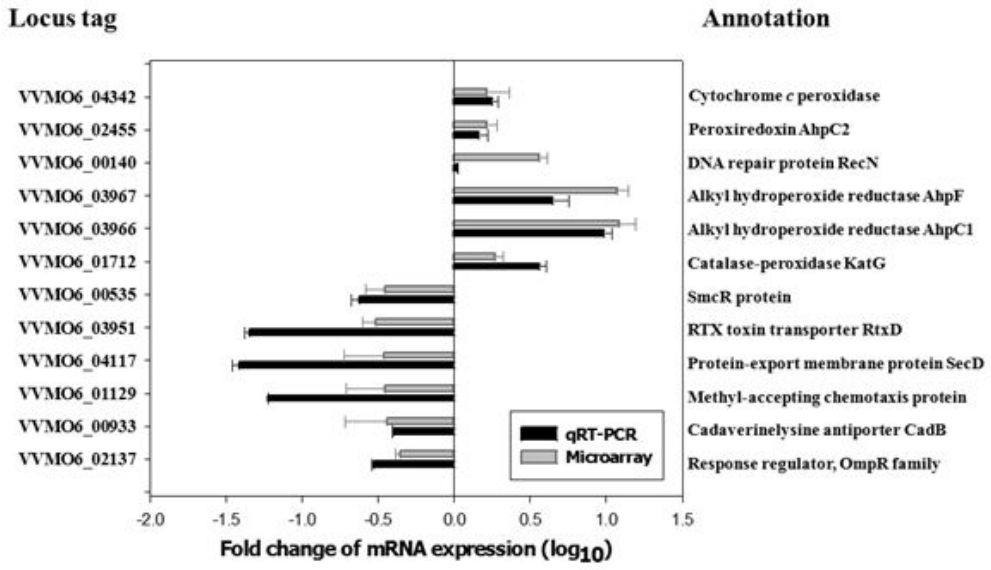

Figure I- 2. Genes induced under H_2O_2 were identified by using Microarray and qRT-PCR

Twelve genes from the pool of the genes regulated under H_2O_2 on the basis of microarray analysis were verified by qRT-PCR. Each column represents the relative mRNA expression level under H_2O_2 versus the wild type. Average and standard errors of the mean (SEM) were calculated from at least three independent experiments, Locus tags are based on the database of the *V. vulnificus* MO6-24/O genome as described in the legend of figure I-1 and the products of the twelve genes are presented on the right.

Table 1. Plasmids and bacterial strains used in this study

Strain or plasmid	Relevant characteristics [a]	Reference or source
Bacterial Strains		
V. vulnificus		
MO6-24/O	Clinical isolate; virulent	Laboratory collection
OH0701	MO6-24/O with *ahpC*1::*nptI*; Km^r	Baek *et al*., 2009
BK081	MO6-24/O with *ahpF*::*nptI*; Km^r	This study
JK115	MO6-24/O with *Δ oxyR*	This study
katG$^-$	MO6-24/O with *katG*::*nptI*; Km^r	K. H. Lee (unpublished)
E. coli		
DH5	*supE44 Δ lacU169 (ϕ80 lacZ* ΔM15*) hsdR17 recA1 endA1 gyrA96 thi-1 relAI*	Laboratory collection
SM10λpir	*thi thr leu tonA lacY supE recA*::RP4-2-Tc::Mu λ *pir*; Km^r; host for π-requiring plasmids; conjugal donor	Miller *et al*., 1988
BL21 (DE3)	*F*$^-$, *ompT*, *hsdS* (r_B^-, m_B^-), *gal* (DE3)	Laboratory collection
Plasmids		
pUC4K	pUC4 with *nptI*; Ap^r, Km^r	Pharmacia
pDM4	Suicide vector; *ori*R6K; Cm^r	Milton *et al*., 1996
pGEM-T easy	PCR product cloning vector; Ap^r	Promega
pRSET A	His-tag protein expression vector; Ap^r	Invitroge
pET22b(+)	His-tag protein expression vector; Km^r	Novagen
pRK415	Inc P *ori*; broad host range vector; *oriT* of RP4; Tc^r	Laboratory collection
pBBRlux	Broad host range vector containing promoterless lux operon; Cm^r	Lenz *et al*., 2004

pJH0311	0.3-kb NruI fragment containing multi-cloning site of pUC19 cloned into pCOS5; Ap^r, Cm^r	Goo *et al*., 2006
pJK1113	Expression vector with the P_{BAD} promoter; Ap^r	Laboratory collection
pMJ0701	pGEM-T easy with *nanA*; Ap^r	This study
pMJ0702	pDM4 with *nanA::nptI* ; Cm^r, Km^r	This study
pMJ0703	pJH0311 with *nanA*; Ap^r, Cm^r	This study
pWK0802	pRSET A with *ahpF*; Ap^r	This study
pWK0704	pRSET A with *ahpC*1; Ap^r	This study
pWK0702	pJH0311 with *ahpC*1*F*; Ap^r, Cm^r	This study
pSS1301	pKJ1113 with *ahpC*1*F*; Ap^r, Km^r	This study
pDY0904	pET22b(+) with oxyR; Km^r	This study
pSS1105	pRK415 with P_{ahpC1} and *ahpC*1*F*; Tc^r	This study
pSS1110	pSS1105 with mutation (-16, T→G) in the P_{ahpC1}; Tc^r	This study
pSS1111	pSS1105 with mutation (-8, T→C) in the P_{ahpC1}; Tc^r	This study
pSS1112	pSS1105 with mutation (+1, G→T) in the P_{ahpC1}; Tc^r	This study
pSS1005	pBBRlux with P_{ahpC1}; Cm^r	This study
pSS1320	pSS1005 with mutation (-16, T→G) in the P_{ahpC1}; Cm^r	This study
pSS1321	pSS1005 with mutation (-8, T→C) in the P_{ahpC1}; Cm^r	This study
pSS1322	pSS1005 with mutation (+1, G→T) in the P_{ahpC1}; Cm^r	This study
pSS1323	pBBRlux with P_{ahpC1} and 136 bp DNA fragment of *ahpC*1 ORF	This study
pSS1324	pBBRlux with P_{ahpC1} and 136 bp DNA fragment of *ahpC*1*F* intergenic region	This study
pSS1325	pBBRlux with P_{ahpC1} and 111 bp DNA fragment of *ahpC*1*F* intergenic region	This study
pSS1326	pBBRlux with P_{ahpC1} and 55 bp DNA fragment of *ahpC*1*F* intergenic region	This study
pSS1327	pBBRlux with P_{ahpC1} and 30 bp DNA fragment of *ahpC*1*F* intergenic region	This study

[a] Ap^r, ampicillin resistant; Km^r, kanamycin resistant; Cm^r, chloroamphenicol resistant; Tc^r, tetracycline resistant.

Table 2. Oligonucleotides used in this study

Oligonucleotide	Oligonucleotide sequence, 5'→3'	Location	Use
AhpC0701	TCAAATAACGCCTTTAGTCCCTCAGG	Chromosomal DNA	Mutant construction
AhpC0704	ATCTAGGCTGACCACTAAACGGAC	Chromosomal DNA	Mutant construction
HIS-AHPC01	CTCGAGATGATTAACACTACTATCAAACCA	Chromosomal DNA	Amplification of *ahpC*1 gene
HIS-AHPC02	AAGCTTTTAGATTTTGCCAACTAGGTC	Chromosomal DNA	Amplification of *ahpC*1 gene
HIS-AHPF01	CTCGAGATGCTAGACCAAGCGATC	Chromosomal DNA	Amplification of *ahpF* gene
HIS-AHPF02	AAGCTTTTAGCCTTGCTTACGAATCAA	Chromosomal DNA	Amplification of *ahpF* gene
AhpC-CP01	GAGCTCCGATGCCAAACCTAACAAACT	Chromosomal DNA	Complementation of *ahpC*1
AhpC-CP02	CCCGGGACATGCCTTTGCTG	Chromosomal DNA	Complementation of *ahpC*1
KatG-CP01	TAATGCTAGCGACAAGGAGCAACACATG	Chromosomal DNA	Complementation of *katG*
KatG-CP02	AGTGGGTACCTTAGATATCGAAGCGATCC	Chromosomal DNA	Complementation of *katG*
AhpC-qRT01	CAGACCGTGCTACTTTCGTTATCG	*ahpC*1	qRT-PCR
AhpC-qRT02	CGTTTGTTCGCCTTCTTTCCATTTAG	*ahpC*1	qRT-PCR
KatG -qRT01	CCTGAAGGTGTAGATGGTAATCCCGACC	*katG*	qRT-PCR
KatG -qRT02	CAGATGGAAGAAGCCGTTATCCCATTG	*katG*	qRT-PCR
AhpC-RE01	CAAACTGGTTGGCAAATCAGCCGT	*ahpC*1	EMSA, Footprinting
AhpC-RE02	CATTTGCCCAATACGTCTTGTTC	Chromosomal DNA	EMSA, Footprinting
KatG-RE01	GGTGCTATACCGTTAATCAGGCAGATAAGTTC	*katG*	EMSA, Footprinting
KatG-RE02	GCGACATTGGATGAGTTTGAAGAAGTGG	Chromosomal DNA	EMSA, Footprinting
AhpC-PR01	CGACTGAACTTGGTGACCTAGCAGACC	*ahpC*1	Construction of *ahpC*1 probe
AhpC-PR02	TTGCGTAGTAGGTCTTCTGCGTCACG	*ahpC*1	Construction of *ahpC*1 probe
AhpF-PR01	CACACTGTGATGGCCCTTTGT	*ahpF*	Construction of *ahpF* probe
AhpF-PR02	TACCATCACCAACCACTTCGG	*ahpF*	Construction of *ahpF* probe
RACE-ASP	CAAAGCAGTGTTCATTCATCGCC	3'RACE adaptor	3'RACE
RACE-GSP	CAACTGACACGCATTTC	*ahpC*1	3'RACE

Oligonucleotide	Oligonucleotide sequence, 5'→3'	Location	Use
AhpC-LR01	AAAAGAGCTCCACAACGCTATCACAC	Chromosomal DNA	Construction of *ahp-lux* reporter
AhpC-LR02	GACTCAGATCCGAAAGTGAAGTCCGC TG	Chromosomal DNA	Construction of *ahp-lux* reporter
AhpC-LR03	GATCTGAGTCTCATTTGCGTTGATTAC CC	Chromosomal DNA	Construction of *ahp-lux* reporter
AhpC-LR04	GCTTGGTCACTAGTACTCGAATACCT TTATAGTTT	Chromosomal DNA	Construction of *ahp-lux* reporter
AhpC-LR05	CATATAGTACTAGTAAATTGGAGAGCG GTCACTC	Chromosomal DNA	Construction of *ahp-lux* reporter
AhpC-LR06	AGCATTACTAGTGTCAAGTAAAACGC CCG	Chromosomal DNA	Construction of *ahp-lux* reporter
AhpC-LR07	CCGGCACTAGTTTTAACTTAAGGGGT AATC	Chromosomal DNA	Construction of *ahp-lux* reporter

Chapter II.

Characterization of *Vibrio vulnificus* *ahpC*1 and *katG* induced under oxidative stress

II-1. Introduction

Aerobic microorganisms inevitably encounter ROS generated as a result of respiration, aerobic metabolism and environmental stresses. In addition, when microbial infection occurs, pathogenic bacteria are especially attacked by oxidative stress as a crucial host defense mechanism (Miller and Britigan, 1997). To reduce ROS levels and oxidative stress generated from these various ways, bacteria induce the expression of antioxidant defense enzymes, including alkyl hydroperoxide reductase (*ahpC*) that scavenges alkyl and lipid hydroperoxides (Seaver and Imlay, 2001a) and superoxide dismutases (manganese superoxide dismutase, *sodA*; iron superoxide dismutase, *sodB*; copper-zinc superoxide dismutase, *sodC*) (Carlioz and Touati, 1986). The expression levels of hydroperoxidases (catalase) are also increased under H_2O_2 induced oxidative stress (Neidhardt *et al*., 1996).

Peroxiredoxins are a family of cysteine-based peroxidases able to reduce H_2O_2 and organic peroxides by the use of reducing equivalents (or reductants) derived from thiol-containing donor molecules such as glutathione, thioredoxin, and alkyl hydroperoxide reductase subunit F (AhpF). AhpC (alkyl hydroperoxide reductase subunit C), one of the best

characterized peroxiredoxins, forming a novel NAD(P)H-dependent peroxide reductase system with AhpF, was originally identified from *Escherichia coli* and *Salmonella typhimurium* (Christman *et al*., 1985; Greenberg and Demple, 1988; Jacobson *et al*., 1989). AhpC and its homologues carrying two conserved cysteinyl residues near its N- and C-termini, respectively, are ubiquitous proteins and expressed in a wide range of eubacteria (Wood *et al*., 2003; Poole, 2005).

Most bacteria contain catalase, although serptococcim, enterococci and leuconostocs do not. All catalase with heme as a cofactor catalyze the typical disproportionation reaction, while some exhibit an additional peroxidatic activity. Catalases with only catalatic activity are called monofunctional catalases, and those with both catalatic and peroxidatic activities are referred to as bifunctional catalases or catalase-peroxidases (Mishra and Imlay, 2012). *E. coli* possesses two catalase genes, *katG* and *katE*, encoding a periplasmic catalase (HPI) and a cytoplasmic catalase (HPII), respectively. These enzymes function as H_2O_2 scavengers, protecting cells from H_2O_2 toxicity. Whereas *katG* is a bifunctional catalase induced by hydrogen peroxide, *katE* is a monofunctional catalase induced by entry into the stationary phase (Storz and Zheng, 2000; Mulvey *et al*., 1990).

The pathogenic marine bacterium *Vibrio vulnificus* is the causative agent of food-borne diseases such as life-threatening septicemia and possibly gastroenteritis in individuals with underlying predisposing conditions (for recent reviews, see Linkous and Oliver, 1999; Strom and Paranjpye, 2000; Jones and Oliver, 2009). Although, like many other pathogenic bacteria, *V. vulnificus* has to cope with oxidative stresses in host environments to ensure developing illness, only a few studies have addressed the molecular mechanisms by which the bacterium can survive under oxidative stresses (Park *et al.*, 2004; Kang *et al.*, 2007). Accordingly, as an effort to characterize the molecular mechanisms involved in oxidative stress resistance, a transcriptome analysis was performed using the *V. vulnificus* Whole Genome Twin-Chip in the present study. Throughout the microarray experiment, *ahpC*1 and *katG*, homologues of *E. coli ahpC* and *katG*, respectively, were identified among the genes specifically induced by exposure to H_2O_2. The purified AhpC1 reduced H_2O_2 and *t*-BOOH in the presence of AhpF and NADH as a hydrogen donor. *katG* also had the antioxidant function to protect bacteria from H_2O_2 and the activity of a catalase. The function of the AhpC1 protein during an infectious process was further accessed by constructing an isogenic *ahpC*1 mutant of *V. vulnificus* and applying the molecular version of Koch's postulates (Falkow, 1988). The

possible roles of AhpC1 and KatG in virulence of *V. vulnificus* have been demonstrated by comparing the virulence of the mutant with that of its parental wild type in *in vitro* cell culture and in mice.

II-2. Materials and Methods

II-2-1. Strains, plasmids, and culture media

The strains and plasmids used in this study are listed in Table 1. Escherichia coli strains used for plasmid DNA replication or the conjugational transfer of plasmids were grown in Luria-Bertani (LB) broth or in LB broth containing 1.5% (wt/vol) agar. Unless noted otherwise, the *V. vulnificus* strains were grown in Luria-Bertani (LB) medium supplemented with 2.0% (w/v) NaCl (LBS). All the media components were purchased from Difco (Detroit, MI), and the chemicals were purchased from Sigma (St. Louis, MO).

II-2-2. Identification of *V. vulnificus ahpC*1 and *katG*

To identify genes induced upon exposure to oxidative stress, the *V. vulnificus* cells grown to A_{600} of 0.5 in LBS were exposed to 250 μM hydrogen peroxide (H_2O_2) for 30 min. A transcriptome analysis was performed using the *V. vulnificus* Whole Genome Twin-Chip as described previously (Jeong *et al*., 2008), and then transcription profiles from the *V. vulnificus* cells exposed either to H_2O_2 or LBS alone were compared. Among the genes of which expression was more induced in the cells exposed to

H_2O_2 (data not shown), *ahpC*1 encoding a peroxiredoxin and *katG* encoding a catalase were selected for further characterization.

II-2-3. Generation of the *ahpC*1 mutant by allelic exchange

The *ahpC*1 gene in pMJ0701 that was inactivated *in vitro* by inserting the 1.2 kb DNA fragment carrying *nptI* encoding for aminoglycoside 3'-phosphotransferase and conferring resistance to kanamycin (Oka *et al*., 1981) into a unique *BamH*I site present within the ORF of *ahpC*1. The 2.1 kb *ahpC*::*nptI* cartridge from the resulting construction (pMJ0702) was liberated and ligated with *Sac*I- *Sph*I digested pDM4 (Milton *et al*., 1996), forming pMJ0703. *E. coli* SM10 *λ pir, tra* (Miller and Mekalanos, 1988) harboring pMJ0703 was used as a conjugal donor to *V. vulnificus* MO6-24/O. The conjugation and isolation of the transconjugants were conducted using the methods previously described (Lee *et al*., 2007, Oh *et al*., 2009).

II-2-4. Survival of the *V. vulnificus* strains under hydrogen peroxide

V. vulnificus wild type, *ahpC*1 mutant and *katG* mutant were grown in the LBS broth until stationary phase. After three strains were treated with 30mM H_2O_2, bacterial cells were determined by counting colony forming units (CFU) on LBS agar plates.

II-2-5. Spotting assay

The ability of the *V. vulnificus* wild type, *ahpC*1 mutant, *katG* mutant and each complemented strain to survive under oxidative stress was assayed by measuring growth on the LBS agar medium containing 250 μM H_2O_2. The ability of the wild type, *ahpC*1 mutant and *katG* mutant to survive under either 60 μM *tert*-butyl hydroperoxide (*t*-BOOH) or 30 μM cumene hydroperoxide (CHP) was confirmed by the same way. Various oxidants were prepared and added to the LBS agar medium by using previously described procedures (Jeong *et al*., 2000). Equal number of the strains grown to log phase (A_{600} of 0.5) were serially diluted from 10 to 1 x 10^4 folds and then 10 μl of the diluted cultures were spotted onto the medium.

II-2-6. Overexpression and purification of *V. vulnificus* AhpC1 and AhpF

The coding region of *ahpC*1 was amplified using the chromosomal DNA of *V. vulnificus* MO6-24/O as a template and oligonucleotide primers, HIS-AHPC01 and HIS-AHPC02 (Table 2). The 0.6 kb PCR product was subcloned into a 6× Histidine tagging expression vector, pRSET A (Invitrogen, Carlsbad, CA). The resulting plasmid, pWK0704, encoded AhpC1 with a 6× His tag at the amino terminus (Table 1). The His-tagged

AhpC1 protein was then expressed in *E. coli* BL21 (DE3), and the protein was purified by affinity chromatography according to the manufacturer's procedure (Qiagen, Valencia, CA). In a similar way, the expression and purification of His-tagged AhpF were fulfilled using pWK0802 (Table 1), carrying the *V. vulnificus ahpF* gene amplified using oligonucleotide primers, HIS-AHPF01, HIS-AHPF02 (Table 2).

II-2-7. Peroxide reductase activity of AhpC1

The peroxide reductase (peroxidase) activity of purified AhpC1 was determined according to the method of Wang *et al*. (Wang *et al*., 2005). The reaction mixture contained 50 mM potassium phosphate (pH 7.0), 1 mM EDTA, 150 mM ammonium sulfate, 100 μM peroxides (H_2O_2 or *t*-BOOH), and either 2 μM AhpC, 0.2 μM AhpF, or both proteins. The reaction was initiated by adding NADH (200 μM) to 200 μl of the mixture and carried out at room temperature. The oxidation of NADH in the resulting mixture was determined by measuring the decrease of absorbance at 340 nm (A_{340}) for time intervals. The protein concentrations were determined by the method of Bradford (Bradford, 1976), with bovine serum albumin as the standard.

II-2-8. Detection of catalase by native gel electrophoresis

Cellular extracts of *V. vulnificus* derived from exponential and stationary phase cells were prepared by B-fer protein extraction reagent (Thermo Fisher Scientific, Rockford, IL). The protein concentrations were determined by the method of Bradford (Bradford, 1976) with bovine serum albumin as the standard. After separation on an 8% nondenaturing polyacrylamide gel, 0.003% H_2O_2 was soaked into the gel. The location of catalase was visualized by staining the gel with a solution containing 1% $K_3Fe(CN)_6$ and 1% $FeCl_3$.

II-2-9. Cytotoxicity assay

Cytotoxicity assays were performed using INT-407 (ATCC CCL-6) human intestinal epithelial cells. The preparation of the INT-407 cells and infection with the bacterial cultures were performed in a 96-well tissue culture plate (Nunc, Roskilde, Denmark) as previously described (Park *et al*. 2006). The cytotoxicity was then determined by measuring the activity of lactate dehydrogenase (LDH) released in the supernatant using a Cytotoxicity Detection Kit (Roche, Mannheim, Germany), and expressed using the total LDH activity released from the cells completely lysed by 1% Triton-X 100 as 100%.

II-2-10. Determination of mouse mortality

Mouse mortalities from the wild type *ahpC*1 mutant and *katG* mutant were compared using ICR mice (specific pathogen free; Seoul National University), as described elsewhere (Kim *et al*., 2009). The *V. vulnificus* strains grown in LBS broth at 30°C were harvested and suspended in phosphate-buffered saline (PBS) to the appropriate concentrations. Groups (n_10) of 8-week-old normal female mice, with an iron-dextran pretreatment, were injected intraperitoneally with 0.1 ml of the bacterial suspensions, and mouse mortalities were recorded for 20 h. All manipulations of mice were approved by the Institute of Laboratory Animal Resources of Seoul National University.

II-2-11. Data analyses

Averages and standard errors of the mean (SEM) were calculated from at least three independent trials. Mouse mortality was evaluated using the log rank test program (http://bioinf.wehi.edu.au/software/russell/logrank/).

II-3. Results

II-3-1. Construction and confirmation of the *V. vulnificus ahpC*1 mutant

To further characterize the function of *V. vulnificus* AhpC1, an isogenic *ahpC*1 mutant was constructed by allelic exchange (Fig. II-1A). A double crossover, in which the wild-type *ahpC*1gene was replaced with the *ahpC*1::*nptI* allele, was confirmed by a PCR using a pair of primers, AhpC 0701 and AhpC 0704 (Table 2). The PCR analysis of the genomic DNA from MO6-24/O with the primers produced a 0.9 kb fragment (Fig. II-2B), whereas the genomic DNA from the *ahpC*1::*nptI* mutant resulted in an amplified DNA fragment approximately 2.1 kb in length. The 2.1 kb fragment was in agreement with the projected size of the DNA fragment containing the wild-type *ahpC*1 (0.9 kb) and the *nptI* gene (1.2 kb). The *V. vulnificus ahpC*1 mutant chosen for further analysis was named OH0701 as shown in Figure II-2B (Table 1).

II-3-2. Effects of the *ahpC*1 and *katG* mutation on the survival of *V. vulnificus* under H_2O_2

The number of viable cells of *V. vulnificus* wild type, *ahpC*1 mutant and *katG* mutant strains under 30 mM H_2O_2 were determined by CFU counting

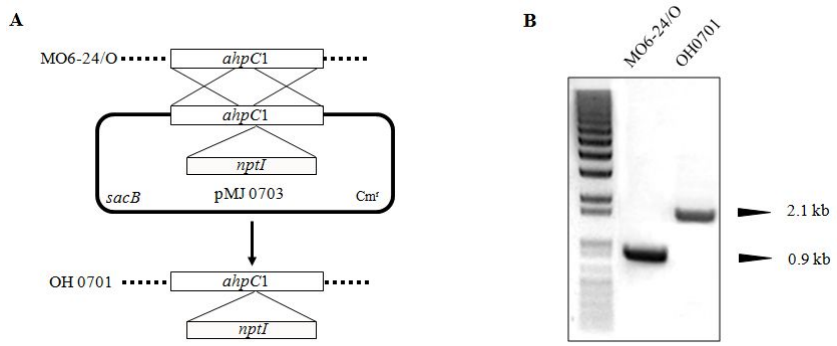

Figure II- 1. Allelic exchange procedure and construction of the *ahpC*1*::nptI* isogenic mutant

(A) Double homologous recombination between strain MO6-24/O and plasmid pMJ0703 led to an interruption of the *ahpC*1 gene and resulted in the construction of the mutant OH0701. The dashed lines represent the bacterial chromosome; the full line, the plasmid DNA; the open box, the target *ahpC*1 gene; the shaded box, the *nptI* gene; and the large Xes, genetic crossing over. Abbreviations; *sacB*, levansucrase gene; Cm^r, chloramphenicol resistance gene. (B) PCR analysis of MO6-24/O and the isogenic mutant OH0701 generated by allelic exchange. Molecular size markers (1kb plus DNA ladder, Invitrogen, Carlsbad, CA) and PCR products are indicated.

and compared at different incubation times as indicated (Fig. II-2A). Whereas the cells of wild type were found to have decreased 3 log CFU/ml after 10 min, that of *ahpC*1 mutant dropped 4 log CFU/ml at the same time, indicating that AhpC1 is responsible for survival of *V. vulnificus* under H_2O_2. When compared with CFU of wild type, that of *katG* mutant significantly decreased (5 log CFU/ml) under 30 mM H_2O_2. These results suggested that the susceptibility of *katG* mutant to H_2O_2 is higher than that of wild type and *ahpC*1 mutant. In order to confirm these results, spotting assay was performed. When spotted on LBS plates supplemented with 250 μM H_2O_2, the survival of the *ahpC*1 mutant and *katG* mutant was significantly impaired compared to that of wild type. In addition, the survival of *katG* mutant was more reduced than that of *ahpC*1 mutant (Fig. II-2B and C).

Reintroduction of recombinant *ahpC*1 could not complement the decrease of survival of *ahpC*1 mutant under H_2O_2 (data not shown). Therefore, to complement the *ahpC*1 mutation, pWK0702 (Table 1) was constructed by subcloning *ahpC*1*F* amplified by PCR using primers AhpC-CP01 and AhpC-CP02 (Table 2) into the broad host-range vector pJH0311 (Goo *et al*., 2006). The impaired survival of *ahpC*1 mutant under H_2O_2 was restored by the reintroduction of pWK0702 (Fig. II-2B). These results

indicated that the presumed *V. vulnificus ahpC*1 and *ahpF* are organized as a single transcriptional unit as in the *ahpCF* genes of *E. coli* (Zheng *et al*., 2001a), and that both AhpC1 and AhpF are required for survival under H_2O_2. In order to complement the *katG* mutation, pSS1301 (Table 1) was constructed by subcloning *katG* ORF amplified by PCR using primers KatG-CP01 and KatG-CP02 (Table 2) into the broad host-range vector pJK1113 (laboratory collection). The impaired survival of *katG* mutant under H_2O_2 was restored by the reintroduction of pSS1301 (Fig. II-2C), indicating that KatG is responsible for survival under H_2O_2.

II-3-3. Effects of the *ahpC*1 and *katG* mutation on the survival of *V. vulnificus* under organic peroxide

The survival of the wild type was much higher than that of the *ahpC*1 mutant when the strains were cultured on the LBS plates in the presence of either 60 μM *t*-BOOH or 30 μM CHP (Fig. II-3A and B). These results suggested that that the gene product of *ahpC*1, AhpC1, is responsible for the survival of *V. vulnificus* under various oxidative stresses.

The survival of the *katG* mutant under organic peroxide was compared to that of wild type strain in the same way. When spotted on LBS plates supplemented with either 60 μM *t*-BOOH or 30 μM CHP, there was not

discrimination between the survival of the *katG* mutant and that of wild type (Fig. II-3A and B). It indicated that, unlike AhpC1, KatG is not important for the survival of *V. vulnificus* under oxidative stress induced by *t*-BOOH and CHP.

II-3-4. Alkyl hydroperoxide reductase activity of AhpC1

The peroxide reductase activity of AhpC1 was determined by measuring its ability to reduce H_2O_2 and *t*-BOOH with NADH as the reducing agent. When AhpF is omitted from the reaction mixture, AhpC1 alone is not able to reduce the peroxides, and thereby no change in the oxidation of NADH (A_{340}) was observed (Fig. II-4A and B). In contrast, AhpF alone had NADH oxidation activity, demonstrating steady decrease in A_{340}. However, the rate of NADH oxidation increased when AhpC1 and AhpF were present together in the reaction mixture, indicating that the AhpC1 activity of reducing peroxides is dependent on AhpF. With all two proteins present, substrate preference was not observed between H_2O_2 and *t*-BOOH (Fig. II-4A and B). Similar results were obtained in independent experiments using NADPH (data not shown). These results indicated that AhpC1 is a peroxiredoxin and constitutes an alkyl hydroperoxide reductase system with AhpF as a reductant in *V. vulnificus*.

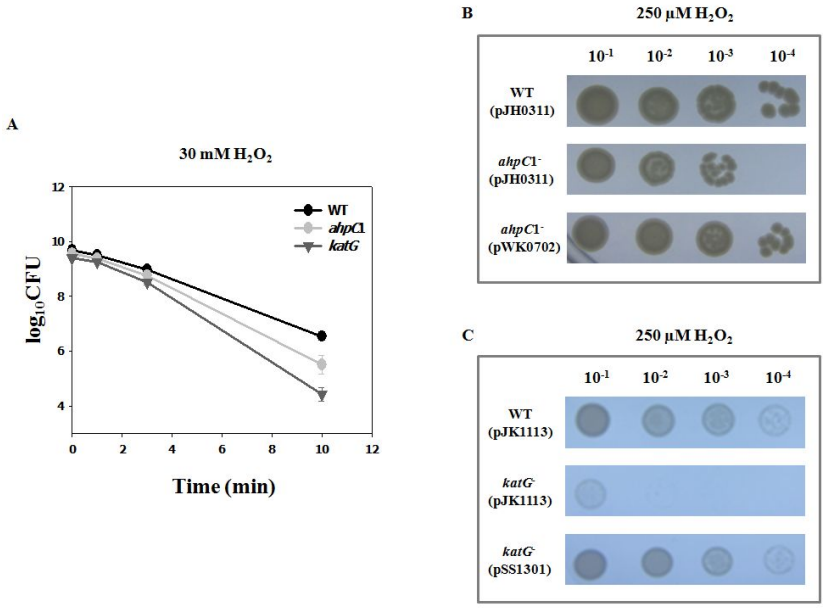

Figure II- 2. Survival of the *V. vulnificus* strains under hydrogen peroxide

(A) Wild type, *ahpC*1 mutant and *katG* mutant cells in the stationary phase were challenged with 30 mM H_2O_2. At several times during exposure, aliquots of each cuture were removed, and the numbers of CFU per milliliter were estimated. (B) Wild-type [WT (pJH0311)], *ahpC*1 mutant [*ahpC*1 (pJH0311)], or complemented strain [*ahpC*1 (pWK0702)] were compared for their ability to grow on LBS plates supplemented with 250 μM H_2O_2. Serial 10-fold dilutions of each culture grown to an A_{600} of 0.5 were spotted on plates as indicated. (C) Wild-type [WT (pJK1113)], *katG* mutant [*katG*

(pJK1113)], or complemented strain [*katG* (pSS1301)] were compared for their ability to grow under the same condition and the experiment was performed by the same way. Each experiment was repeated at least twice.

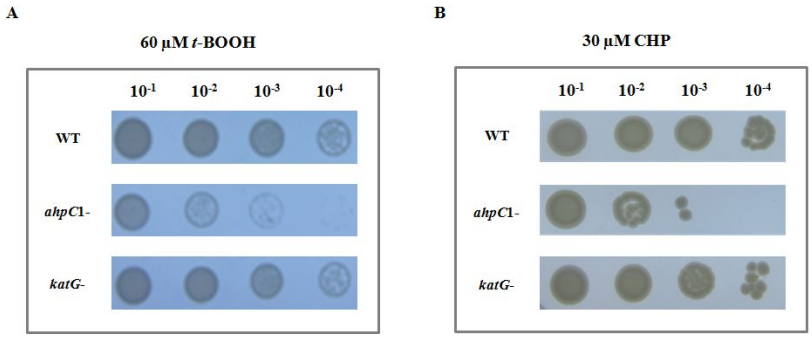

Figure II- 3. Survival of the *V. vulnificus* strains under organic peroxide

Wild type, *ahpC*1 mutant and *katG* mutant were compared for their ability to grow on LBS plates supplemented with either 60 μM *t*-BOOH (A) or 30 μM CHP (B). Serial 10-fold dilutions of each culture grown to an A_{600} of 0.5 were spotted on plates as indicated. Each experiment was repeated at least twice.

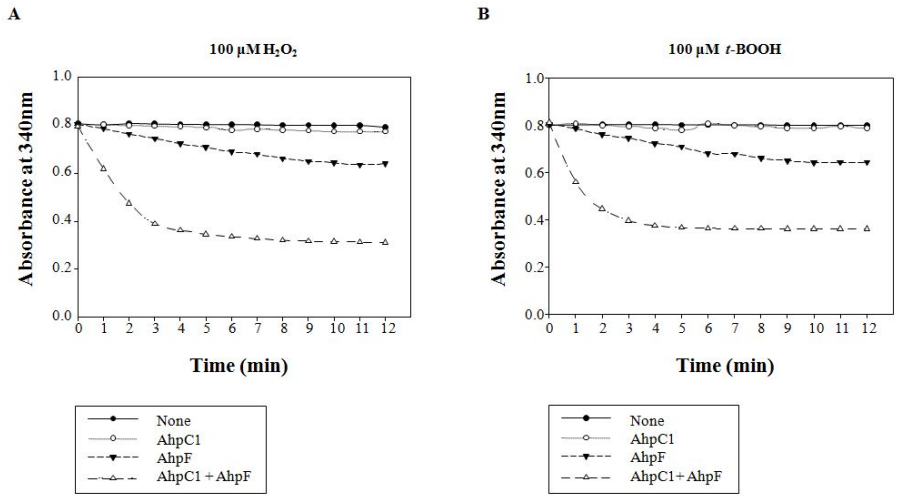

Figure II- 4. NADH and AhpF dependent peroxide reductase assay of AhpC1

The peroxide reductase activity of AhpC1 was determined by monitoring NADH oxidation measured as the decrease in absorbance at 340 nm in the presence of H_2O_2 (A) and *t*-BOOH (B) as indicated. NADH, AhpC1, and AhpF were omitted from the reaction mixture as a negative control (None). Either AhpC1 or AhpF alone, or both proteins are added to the reaction mixture as indicated. Details are in Materials and Methods. Each experiment was repeated at least three times and represents mean of the experiments.

II-3-5. Detection of catalase by native gel electrophoresis

Presence of catalase in the wild type was confirmed by native gel staining for the catalase activity. Electrophoresis was performed using the cellular extracts from cells treated with H_2O_2 in the various phases as indicated in Fig. II-5B. Staining native gel revealed the presence of a single catalase band in the cellular extracts of the wild type. This observation is in agreement with Park *et al*., who have reported that, unlike *E. coli*, *V. vulnificus* possesses only a single gene (*katG*) for catalase (Park *et al*., 2004). In addition, compared to the expression levels of *katG* under various conditions as indicated above, the intensities of catalase bands under the same conditions were shown a similar trend (Fig. II-5A and B).

II-3-6. AhpC1 and KatG are required for cytotoxicity toward epithelial cells *in vitro*

In order to examine the effects of the *ahpC*1 mutation and *katG* mutation on the virulence of *V. vulnificus*, LDH activities from monolayer of INT-407 cells that were infected with 100 μl of suspension of the wild type, *ahpC*1 mutant and *katG* mutant strains at a different multiplicity of infection (MOI) and incubated for 1.5 h were determined (Fig. II-6A and B). The *ahpC*1 mutant exhibited much less LDH releasing activity and the level of

LDH activity released from INT-407 cells infected with *ahpC*1 mutant at a MOI of 10 was almost 3-fold less than that from the cells infected with wild type. The *katG* mutant also revealed low LDH releasing activity and the level of LDH activity released from INT-407 cells infected with *katG* mutant at MOI of 20 was about 2-fold less than that from the cells infected with wild type. The lower LDH activities were restored to the level released from the cells infected with wild type, when the cells were incubated with each complemented strain (Fig. II-6A and B).

II-3-7. Virulence of *ahpC*1 and *katG* in mice

The roles of the *ahpC*1 and *katG* genes in virulence were also examined using a mouse model, and survival curves of mice injected intraperitoneally with either the *ahpC*1 mutant or *katG* mutant or the parental wild type at doses of 5×10^2 CFU were monitored for 20 h (Fig. II-7A and B). The results showed that the deaths of mice injected with the *ahpC*1 mutant and *katG* mutant were consistently and significantly delayed (P_0.05; log rank test) compared to those of mice injected with the parental wild type. Therefore, in the mouse model of intraperitoneal infection, the *ahpC*1 and *katG* mutant appeared to be significantly less virulent than its parental wild type. As such, these results indicated that the *V. vulnificus* AhpC1 and KatG are apparently

important for the pathogenesis of the bacterium.

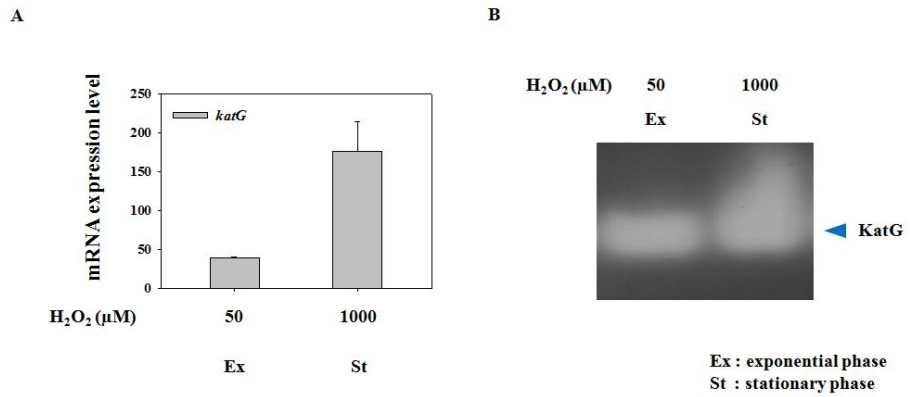

Figure II- 5. The expression pattern of *katG* and the catalase activity of KatG under hydrogen peroxide

(A) The RNA was isolated from *V. vulnificus* wild type which had been treated with H_2O_2 as indicated in the exponential or stationary phase. The expression levels of *katG* form the whole mRNA were detected. (B) Crude extracts (50 μg) prepared from *V. vulnificus* in the exponential or stationary phase which had been treated with H_2O_2 as indicated were loaded into 8% nondenaturing gel, and the KatG activities were examined.

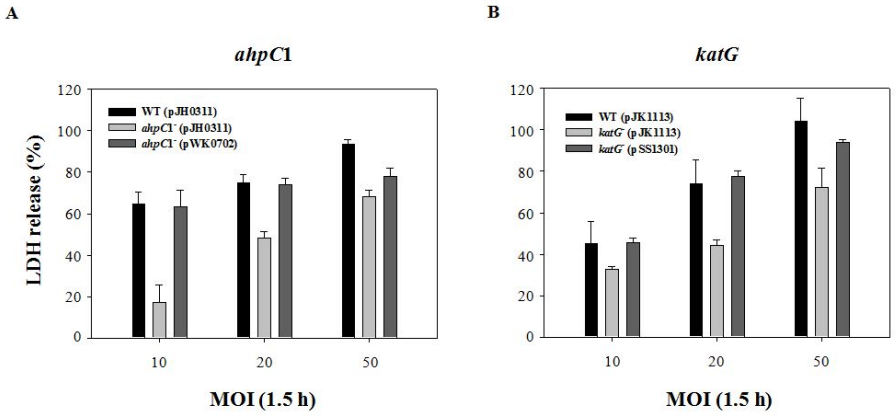

Figure II- 6. Effects of *ahpC*1 and *katG* mutation on virulence of *V. vulnificus* towards INT-407 cells

INT-407 cells were infected with the *V. vulnificus* strains at various MOIs for 1.5 h. Thereafter, the cell cytotoxicity was determined by an LDH release assay.

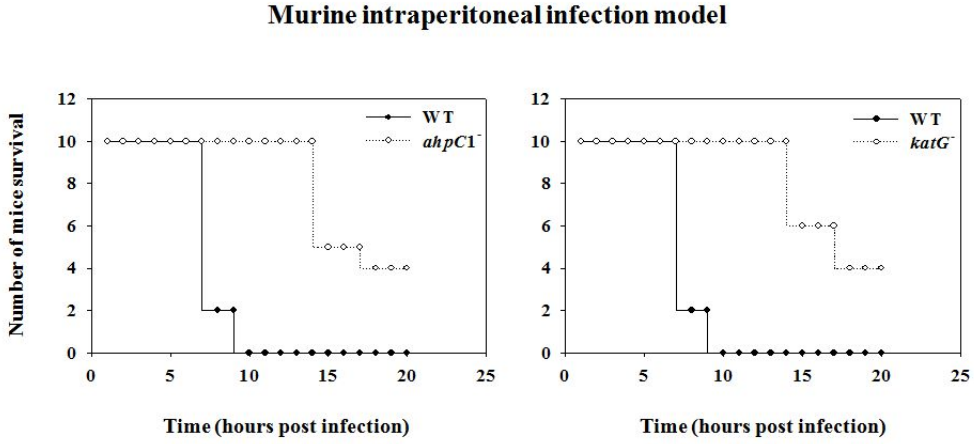

Figure II- 7. Virulence in mice is dependent on *ahpC*1 and *katG*

Eight-week-old specific-pathogen-free female ICR mice were intraperitoneally infected using the wild type, *ahpC*1 mutant or *katG* mutant. Mouse survival was monitored for 20 h.

II-4. Discussion

Like other bacteria, *V. vulnificus ahpC*1 and *katG* are essential for survival under oxidative stress. Interestingly, the survival of *katG* mutant is more susceptible to 30 mM and 250 μM H_2O_2 than that of *ahpC*1 mutant (Fig. II-2A, B and C). There are two reasons to explain the above result. First, it has been reported that the *E. coli* AhpC is able to rapidly degrade low doses of H_2O_2 (<20 μM H_2O_2) while KatG is effective to relatively high level of H_2O_2 (Mishra and Imlay, 2012). That is, AhpC is a primary scavenger of endogenous H_2O_2 while KatG is an important for exogenous H_2O_2 because the rate of endogenous H_2O_2 produced by *E. coli* is lower than 14 μM /s (Seaver and Imlay, 2001a). Therefore it is predicted that the above result is because of the relatively high level of H_2O_2. Second, the expression of *V. vulnificus katG* is much higher than that of *ahpC*1 in stationary phase, on the contrary to the expression levels of *ahpC*1 and *katG* in exponential phase (data not shown). Thus the survival of *katG* mutant is much sensitive to H_2O_2 than that of *ahpC*1 mutant because KatG is predicted a major scavenger in stationary phase.

Although the *katG* mutant is highly susceptible to H_2O_2 than the *ahpC*1

mutant, KatG is not responsible for survival under organic hydroperoxides (Fig. II-3A and B). It has been known that catalase has characteristic deep burial of heme, which can be accessed by through a narrow channel. The narrowness of the channel blocks the entry of molecules larger than H_2O_2 and thus provides substrate specificity. Thus catalase is not able to degrade organic hydroperoxides (Mishra and Imlay, 2012).

Alkyl hydroperoxide reducase system, AhpCF, of Gram-negative bacteria, provides an important protection against peroxides in the environments and within host. AhpCF consists of a catalytic subunit C (AhpC, peroxiredoxin) and a reductase subunit (AhpF). The *ahpC* gene has been highly conserved and can be found in the sequence databases of most completed genomes (Poole, 2003), indicating that protection against ROS by AhpC and its homologues are critical to many organisms. Bacterial AhpCs in *E. coli* and *S. typhimurium* are two cysteinyl peroxiredoxins and their catalytic properties are well characterized biochemically (Poole, 2005). The enzymes utilize a cysteinyl residue at the catalytic site in the N-terminal region for hydroperoxide reduction, leading to formation of a sulfenic acid derivative of the cysteine. The sulfenic acid then reacts with a second cysteine in the C-terminal region to generate an intersubunit disulfide bond

in a dimeric form of AhpC. This disulfide bond in AhpC is subsequently reduced to regenerate the active AhpC by a pair of cysteines of AhpF. The resulting oxidized AhpF is reduced by electron transfer cascade from an AhpF-bound flavin moiety, and then finally from NADH (Jönsson *et al*., 2007). *V. vulnificus* AhpC1 carries two cysteines at the 45th and 164th residues and shows 78% similarity in amino acid sequences with the AhpCs of *E. coli* and *S. typhimurium* (data not shown). In addition, *V. vulnificus* AhpC1 requires AhpF and NADH as reductants for optimum peroxide reduction (Fig. II-4A and B). All these combined indicates that catalytic properties of AhpC1 are also similar with those of the *E. coli* and *S. typhimurium* AhpCs.

KatG and KatE also provide an important protection against peroxides in the environments and within host. Although there are ORF homologous to both *katG* and *katE* in the genome of *V. vulnificus*, unlike *E. coli*, the catalase activity of *V. vulnificus* KatE was not detected (Park *et al*., 2004; Fig. II-5B). In order to determine the expression of *katE* at the transcriptional level, qRT-PCR was performed using the RNA derived from *V. vulnificus* wild type in the various condition and phase. However there was no evidence of the expression of *katE* (data not shown). It has not been clear why *V. vulnificus*

katE is not expressed or in what condition *katE* is expressed until the present time.

It has been generally accepted that virulence factors of infecting microorganisms include all those factors contributing to survival and multiplication on or within host as well as to disease (Mekalanos, 1992). Plants and animals possess mechanisms to specifically generate ROS as a defense against microbial invasion (Storz and Zheng, 2000), and phagocyte-derived ROS and their role in host defense have been biochemically and cytologically well characterized (Miller and Brightigan, 1997). In response, microorganisms have developed elaborate protection system not only to avoid contact with phagocyte-derived ROS but also to defend themselves from injury by ROS encountered. The relationship between ROS resistance of pathogenic bacteria and their virulence in the pathogenesis has been well documented. As an example, *S. typhimurium* carrying mutations in genes essential for protecting against the toxicity of ROS are hypersusceptible to macrophage killing, and show attenuated virulence in mice (Fang *et al*., 1999). Therefore, it is conceivable that factors contributing to protecting against the deleterious effects of ROS are important for virulence of pathogenic bacteria.

The diseases resulting from infection with *V. vulnificus* are remarkable as regards their invasive nature, ensuing severe tissue damage, and rapidly fulminating course (Linkous and Oliver, 1999; Strom and Paranjpye, 2000; Jones and Oliver, 2009). This multifaceted nature of pathology of the diseases indicates that numerous virulence factors are typically involved in pathogenesis of the organism. To investigate whether capability of ROS resistance plays an important role as a virulence factor in the pathogenesis of *V. vulnificus*, the *V. vulnificus ahpC*1 mutant and *katG* mutant showing increased sensitivity to peroxides were constructed and provided, respectively. When compared to wild type, the *ahpC*1 mutant and *katG* mutant were less toxic to intestinal epithelial cells *in vitro*, and also show significantly diminished virulence in mice as measured by their abilities to cause death. In addition, the growth rate of the *ahpC*1 mutant in the INT-407 tissue cultures was significantly lower than that of the wild type (Baek *et al*., 2009). As a conclusion, these results combined suggest that AhpC1, KatG and the capability of protection against ROS toxicity could contribute to the pathogenesis of *V. vulnificus* by assuring survival and multiplication during infection rather than directly aggravating damage or injury of the host.

II-5. Acknowledgements

Thank Dr. Kyu-Ho Lee for providing *V. vulnificus katG* mutant from his laboratory.

Chapter III.

Regulation of the expression of *ahpC*1 and *katG* by *Vibrio vulnificus* OxyR

III-1. Introduction

For many microorganisms, resistance to oxidative stress is a good strategy for their survival. This has to be used by pathogenic bacteria to facilitate infection and counter host defense mechanism, since host species generate ROS as a host defense system (Battistoni *et al*., 2000, Janssen *et al*., 2003). It has been well studied that pathogenic bacteria have inducible responses that protect against oxidative damage. These antioxidant defense systems have been characterization in *E. coli* (Storz and Imlay, 1999).

OxyR is a LysR-type redox sensing transcriptional regulator that is generally found in Gram-negative bacteria (Schell, 1993). It contains a conserved N-terminal helix-turn-helix DNA binding domain, recognition and response domain which senses the regulatory signal, and a C-terminal domain that functions in multimerization and activation (Morikawa *et al*., 2006). OxyR plays a primary role in the response of peroxide stress and activates its regulon having antioxidant function to maintain the intracellular redox homeostasis (Antelmann and Helmann, 2011). Hydrogen peroxide induces the conformational change in the OxyR structure through the oxidation of OxyR at a specific “sensing” cysteine residue and formation of

an intramolecular disulfide bond with both sensing and resolving cysteine residues (Seaver and Imlay, 2001b). The oxidized OxyR then induces the expression of antioxidant genes, including katG (hydroperoxidase I), ahpCF (alkylhydroperoxidase), gorA (glutathione reductase), grxA (glutaredoxin I), and oxyS (a regulatory RNA) (Zheng *et al*., 1999; Zheng *et al*., 2001b).

OxyR can function not only as an activator under oxidized condition but also as a repressor under reduced condition (Christman *et al*., 1989), because oxidized (ox-OxyR) and reduced (red-OxyR) forms of OxyR adopt different conformational states that have different promoter sequence recognition. Generally, the DNA binding contacts of the ox-OxyR shift to contact four major grooves, while the red-OxyR contacting two pairs of major grooves separated by one helical turn (Toledano *et al*., 1994). In addition, the four major grooves bound the ox-OxyR are located in the upstream regions of the target promoters of OxyR, while red-OxyR has the binding sites overlapping a RNA polymerase binding region. Thus ox-OxyR is able to activate its regulon, whereas red-OxyR can repress its regulon by blocking the RNA polymerase.

There are ORF homologous to *oxyR* in the genome of *V. vulnificus*. Though it is known that *V. vulnificus* OxyR regulates *ahpC*1 and *katG* genes

like other bacteria, experimental evidence of its regulation has been still limited. In the present study, the expression levels of *ahpC*1 and *katG* in the wild type were compared to not only those in the *oxyR* mutant under H_2O_2 but also those in the C199S-OxyR mutant, mimicking red-OxyR. In addition, EMSA and DNaseI footprinting experiments revealed that *V. vulnificus* OxyR regulated the expression of *ahpC*1 and *katG* by directly binding to their promoters.

III-2. Materials and Methods

III-2-1. Strains, plasmids, and culture conditions

The strains and plasmids used in this study are listed in Table 1. *Escherichia coli* strains used for plasmid DNA replication or overexpression of protein were grown in Luria-Bertani (LB) broth or in LB broth containing 1.5% (wt/vol) agar the *V. vulnificus* strains were grown in Luria-Bertani (LB) medium supplemented with 2.0% (w/v) NaCl (LBS). All the media components were purchased from Difco (Detroit, MI), and the chemicals were purchased from Sigma (St. Louis, MO).

III-2-2. RNA purification and primer extension analysis

Total cellular RNA was isolated from the wild type grown to A_{600} of 0.5 with LBS supplemented with 50 μM H_2O_2, using a high pure RNA isolation kit (Roche, Mannheim, Germany). Primer extension experiments were carried out with SuperScript II RNase H2 reverse transcriptase (Invitrogen, Carlsbad, CA) according to Sambrook *et al*. (Sambrook *et al*., 1989). The AhpC-RE01 and KatG-RE01 (Table 2) were used for end-labeling and located within the coding region of *ahpC*1 and *katG*, respectively. The primers were end-labeled with [γ-^{32}P] ATP using T4 polynucleotide kinase

(New England Biolabs, Beverly, MA). The cDNA products were purified and resolved on a sequencing gel alongside sequencing ladders generated with the same primers used for the primer extension. The nucleotide sequences of *ahpC*1 and *katG* promoter region amplified with pairs of primers were determined using the dideoxy chain termination method with TopTM DNA polymerase (Bioneer, Seoul, Korea) following the manufacturer's protocols. The primer extension products were visualized and quantified using a phosphorimage analyzer (BAS1500; Fuji Photo Film Co., Ltd., Tokyo, Japan) and the Image Gauge (version 3.12) program.

III-2-3. Quantitative real-time PCR

For quantitative real time PCR (qRT-PCR), cDNAs were synthesized with iScriptTM cDNA synthesis kit (Bio-Rad, Richmond, CA), and real time PCR amplification of the cDNAs was performed with the specific primer pairs for *ahpC*1 and *katG* genes, respectively (Table 2). Relative expression levels of the *ahpC*1 and *katG* transcripts were calculated by using the 16 S rRNA expression level as the internal reference for normalization as described previously (Oh *et al*., 2009).

III-2-4. Overexpression and Purification of *V. vulnificus* OxyR

pDY0904 carrying the *oxyR* coding region subcloned into a His6 tagging expression vector, pET-22b (+) (Novagen, Madison, WI), was grown to A_{600} of 0.5 in the LB broth containing 5 mg/ml kanamycin. In order to induction of OxyR protein, 2 mM IPTG was treated into the cell culture media and then the treated cell culture media were incubated for 40 h at 15˚C. After the His-tagged OxyR protein was expressed in *E. coli* BL21 (DE3), it purified by affinity chromatography according to the manufacturer's protocol (Qiagen, Valencia, CA), as described elsewhere (Choi *et al*., 2002).

III-2-5. Electrophoretic mobility shift assay (EMSA)

EMSAs to measure binding of OxyR to the regulatory regions of *ahpC*1 and *katG* were performed as described by Sambrook *et al*. The 400 bp upstream region of *katG*, extending from residues -232 to +168 from the transcription start site of *katG* gene, was amplified by PCR using [γ-^{32}P]-labeled KatG-RE01 and unlabeled KatG-RE02 as the primers (Table 2). The labeled 400 bp DNA (1 nM) fragment was incubated with various concentrations of purified His-tagged OxyR for 30 min at 30˚C in a 20 μl reaction mixture containing 1X binding buffer [25 mM Tris-Cl (pH 8.0), 25 mM KCl, 6 mM $MgCl_2$, 0.5 mM EDTA, 10% glycerol, 0.05% tween 20, and

50 μg/ml BSA]. The 410 bp upstream region of *ahpC*1 was also amplified by PCR using [γ-^{32}P]-labeled AhpC-RE01 and unlabeled AhpC-RE02 as the primers (Table 2). The labeled 410 bp DNA (1.3 nM) fragment was incubated the same way. Electrophoretic analysis was then performed by using a 7% polyacrylamide gel in 0.5X TBE buffer.

III-2-6. DNase I footprinting experiment

DNase I protection assays were performed as described previously (Choi *et al*., 2002) with slight modifications. 15 nM of the same labeled DNA fragments, used for the EMSA, were suspended in 20 μl of reaction solution containing 1X binding buffer described above and various concentrations of OxyR. The reaction mixtures were incubated for 30 min at 30˚C. 20 μl of 10 mM $MgCl_2$ and 5 mM $CaCl_2$ mix were then added to the reaction mixtures and DNase I (New England Biolabs, Beverly, MA) was treated in the 40 μl reaction mixtures with 0.05 U. The samples were then incubated for 30 second at room temperature, the reactions were stopped by the addition of 50 μl of stop solution (phenol/chloroform/isoamyl alcohol, 25:24:1), and the DNA products were purified by ethanol precipitation. The purified DNA products were resolved on a sequencing gel. Gels were processed as described for the primer extension analysis.

III-3. Results

III-3-1. Primer extension and the promoter sequence analysis

The transcription start sites of *ahpC*1 and *katG* were determined by primer extension analysis. Reverse transcripts were identified from primer extension of the RNAs isolated from the wild type cells treated with H_2O_2 in the exponential phase (Fig. III-1A and 2A). The 5' end of the *ahpC*1 transcript was located 47 bp upstream of the translational initiation codon of *ahpC*1 and subsequently designated +1. The sequences for -10 and -35 regions of *ahpC*1 were assigned on the basis of similarity to consensus sequences of the *E. coli* σ^{70} promoter (Fig. III-1B). The transcription initiation site of the *katG* transcript was located 85 bp upstream of the start codon of *katG* and the putative -10 and -35 regions were also predicted (Fig. III-2B). In addition, OxyR binding consensus sequences were detected in the promoter regions of both *ahpC*1 and *katG* (Fig. III-1B and 2B), indicating that OxyR presumably regulates the expression of *ahpC*1 and *katG* in *V. vulnificus*.

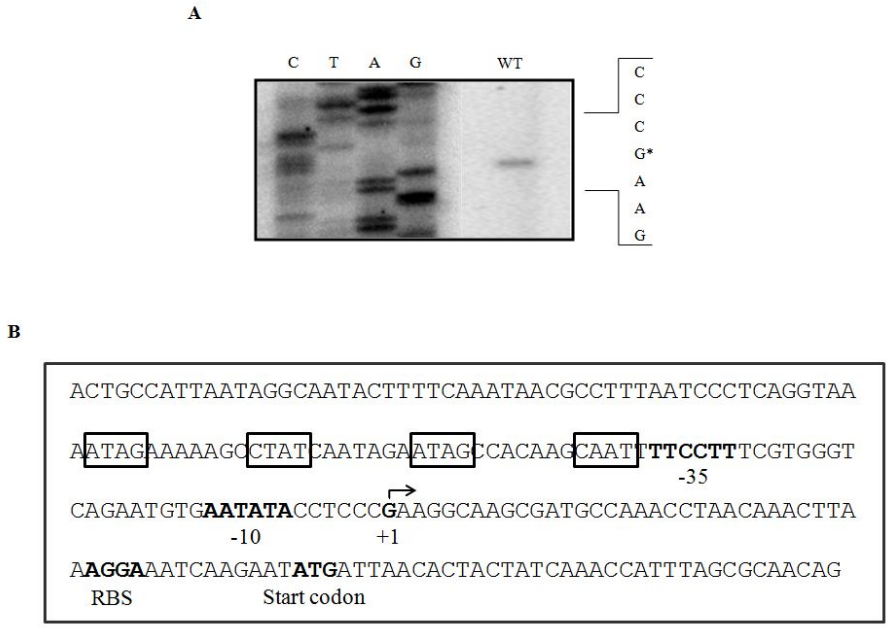

Figure III- 1. Primer extension and sequence analysis of the *ahpC*1 upstream region

(A) The transcription start site was determined by primer extension using the RNA derived from *V. vulnificus* MO6-24/O grown to exponential phase in LBS supplemented with H_2O_2. Lanes G, A, T and C represent the nucleotide sequencing ladder. The transcription start site for P_{ahpC1} is indicated by asterisk. (B) The transcription start site is indicated by a bent arrow. OxyR binding consensus sequences are boxed. The positions of the putative -10 and -35 regions for the P_{ahpC1}, the ATG translation initiation codon, and putative ribosome binding site (RBS) are indicated in bold face type.

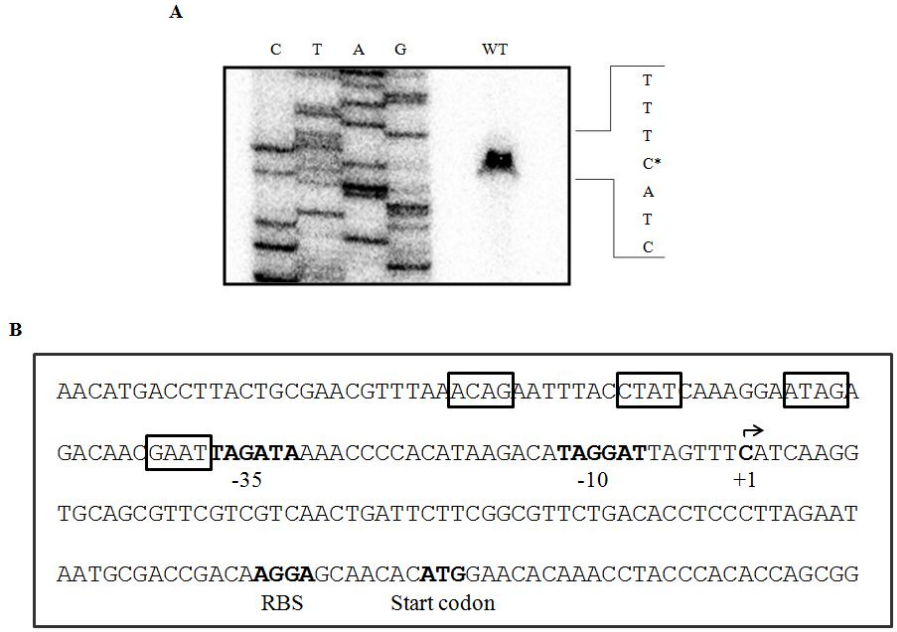

Figure III- 2. Primer extension and sequence analysis of the *katG* upstream region

(A) The transcription start site was determined by primer extension using the RNA derived from *V. vulnificus* MO6-24/O grown to exponential phase in LBS supplemented with H_2O_2. Lanes G, A, T and C represent the nucleotide sequencing ladder. The transcription start site for P_{katG} is indicated by asterisk. (B) The transcription start site is indicated by a bent arrow. OxyR binding consensus sequences are boxed. The positions of the putative -10 and -35 regions for the P_{katG}, the ATG translation initiation codon, and putative ribosome binding site (RBS) are indicated in bold face type.

III-3-2. Transcriptional regulation of *ahpC*1 and *katG* by oxidized OxyR

A qRT-PCR experiment was performed using the RNA isolated from wild type and *oxyR* mutant grown to A_{600} of 0.5 in LBS supplemented with 50 μM H_2O_2. The amounts of *ahpC*1 and *katG* mRNAs in the *oxyR* mutant were significantly decreased as compared to those in wild type (Fig. III-3). This result indicated that the expression of *ahpC*1 and *katG* was activated by ox-OxyR.

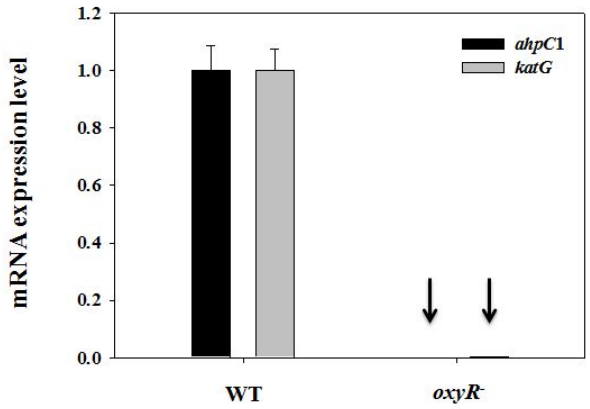

Figure III- 3. The expression of *ahpC*1 and *katG* in the *oxyR* mutant

Whole mRNAs were isolated from *V. vulnificus* wild type and *oxyR* mutant under the condition as described in result III-3-2. The expression levels of *ahpC*1 and *katG* form the whole mRNA were detected. The expression levels of *ahpC*1 and *katG* in wild type were normalized in 1, respectively, and then those in *oxyR* mutant were shown as relative values compared to those in wild type.

III-3-3. EMSA for oxidized OxyR binding to the *ahpC*1 and *katG* regulatory regions

The 410 bp and 400 bp DNA fragments encompassing the *ahpC*1 and *katG* regulatory regions, respectively, were incubated with increasing amounts of ox-OxyR and then subjected to electrophoresis. As shown in Fig. III-4A, the addition of 10 nM ox-OxyR resulted in a shift of the 410 bp DNA fragment to double bands and there was a full-shift single band at a concentration of 80 nM ox-OxyR. In lane 6 to 8, the same, but unlabeled, 410 bp DNA fragment was used as a self-competitor to confirm the specific binding of ox-OxyR to the promoter of *ahpC*1 (P_{ahpC1}). The unlabeled 410 bp DNA competed for the binding of ox-OxyR in a dose-dependent manner (Fig. III-4A). The ox-OxyRs at the indicated concentrations were mixed in the reaction mixture and also bound the promoter of *katG* (P_{katG}) (Fig. III-4B). Unlike the 410 bp DNA fragment, the 400 bp DNA segment was not a full-shift single band at a concentration of 80 nM ox-OxyR, indicating that P_{ahpC1} has higher affinity to ox-OxyR than P_{katG}. These results suggested that ox-OxyR activated the expression of the *ahpC*1 and *katG* by directly binding to their promoters.

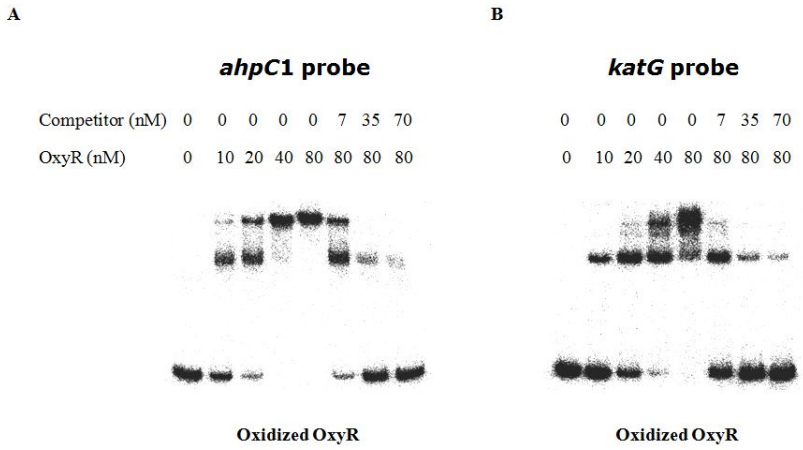

Figure III- 4. Electrophoretic mobility shift assay for oxidized OxyR binding to the *ahpC*1 and *katG* regulatory regions

A 410 bp DNA fragment containing the *ahpC*1 promoter (A) and a 400 bp DNA fragment containing the *katG* promoter (B) were radioactively labeled and then used as DNA probes. The EMSA reactions were performed by adding either 1.3 nM (*ahpC*1) or 1.1 nM (*katG*) of labeled probes and purified OxyR to OxyR binding buffer. For competition analysis, the same, but unlabeled, DNA fragments were used as competitors. Various amounts of the competitor DNAs, respectively, were added to a reaction mixture containing either 1.3 nM or 1.1 nM labeled DNAs prior to the addition of OxyR. In lanes 6 to 8, DNA probes were incubated with OxyR and 7, 35 or 70 nM of the competitor DNAs, respectively, as indicated.

III-3-4. Identification of the oxidized OxyR binding site using DNase I footprinting experiment

To determine the precise location of the ox-OxyR binding site in the *ahpC*1 regulatory region, a DNase I footprinting experiment was performed using the same 410 bp DNA fragment used for the gel shift assays. DNase I footprinting with ox-OxyR revealed a clear protection pattern in the upstream regions of *ahpC*1 from -44 to -80 and from -99 to -147 (Fig. III-5A). The protected region, extending from -44 to -80, was overlapped with a consensus sequence for OxyR binding. In contrast, the protection region, extending from -99 to -147, was not resembled the OxyR binding consensus sequence (Fig. III-5C). In order to define the location of the ox-OxyR binding site in the *katG* regulatory region, a DNase I footprinting was carry out by the same way. A clear protection region by binding of the ox-OxyR in the upstream region of *katG* was located from -36 to -72 (Fig. III-5B) and overlapped with a consensus sequence for OxyR binding. Collectively, these observations confirmed that ox-OxyR functioned as a class I activator and activated the expression of both *ahpC*1 and *katG* by directly binding to specific OxyR binding sites in the upstream regions of *ahpC*1 and *katG*.

A

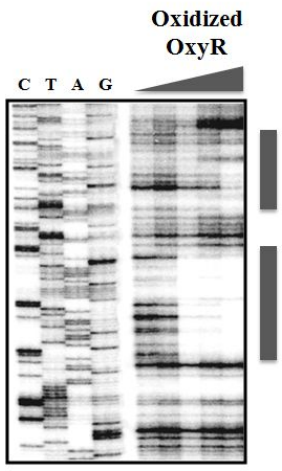

*ahpC*1 probe

B

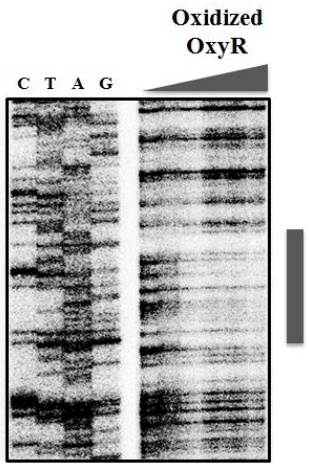

katG probe

C

CTCTTCAGAAAATGGTTCCACAACGCTATCACACCAACAGTACCTATCAAAAC

ACTGCCATTAATAGGCAATACTTTTCAAATAACGCCTTTAATCCCTCAGGTAA

AATAGAAAAAGCCTATCAATAGAATAGCCACAAGCAATT**TTCCTT**TCGTGGGT

-35

CAGAATGTG**AATATA**CCTCCC**G**AAGGCAAGCGATGCCAAACCTAACAAACTTA

-10 +1

A**AGGA**AATCAAGAAT**ATG**ATTAACACTACTATCAAACCATTTAGCGCAACAG

RBS Start codon

D

GTTCCGCTATCTCGACAAAGTGGATGCCATCTTCTCTGACTATCCCGAACGTT

TTATCTAGCGTTCTCCCCTATCAAACCACTCGTTTTCGGATGAGTGGTTTCAA

AACATGACCTTACTGCGAACGTTTAAACAGAATTTACCTATCAAAGGAATAGA

GACAACGAAT**TAGATA**AAACCCCACATAAGACA**TAGGAT**TAGTTTC**A**TCAAGG

-35 -10 +1

TGCAGCGTTCGTCGTCAACTGATTCTTCGGCGTTCTGACACCTCCCTTAGAAT

AATGCGACCGACA**AGGA**GCAACAC**ATG**GAACACAAACCTACCCACACCAGCGG

RBS Start codon

Figure III- 5. DNase I protection analysis for identification of oxidized OxyR binding site and sequence analysis of the *ahpC*1 and *katG* upstream regions

(A) The ^{32}P-labeled 410 bp *ahpC*1 regulatory region was incubated with increasing amounts of ox-OxyR and then digested with DNase I. Lane 1, no OxyR added; lanes 2 to 5, ox-OxyR at 100, 200, 300, and 400 nM, respectively. (B) The ^{32}P-labeled 400 bp *katG* regulatory region was incubated with increasing amounts of ox-OxyR and then digested with DNase I. Lane 1, no OxyR added; lanes 2 to 6, ox-OxyR at 100, 200, 300, 400, and 500 nM, respectively. Lanes G, A, T, and C represented the nucleotide sequencing ladder. The protection regions in the presence of ox-OxyR were indicated by grey boxes. (C and D) The transcription start site was indicated by a bent arrow. The positions of the putative -10 and -35 regions, the ATG translation initiation codon, and putative ribosomal binding sequence (RBS) were printed in bold letters. The sequences proposed for the binding sites of ox-OxyR were shown in solid under lines. The conserved nucleotide sequences for the binding of OxyR were indicated by boxes.

III-3-5. EMSA for reduced OxyR binding to the *ahpC*1 and *katG* regulatory regions

The *ahpC*1 and *katG* DNA probes used in EMSA for ox-OxyR were incubated with increasing amounts of red-OxyR and then carried out electrophoresis. Like ox-OxyR, EMSA for red-OxyR also revealed a shift of the *ahpC*1 and *katG* probes. In addition, the patterns of shift bands in EMSA for red-OxyR were similar to those in EMSA for ox-OxyR. In lane 6 to 8, through a self-competitor, the specific binding of red-OxyR to the both P_{ahpC1} and P_{katG} was also confirmed (Fig. III-6A and B). These results indicated that red-OxyR bound the regulatory regions of the *ahpC*1 and *katG* and presumably regulated the expression of both two genes.

III-3-6. Identification of the reduced OxyR binding site using DNase I footprinting experiment

To determine the precise locations of the red-OxyR binding site in the *ahpC*1 and *katG* regulatory regions, a DNase I footprinting experiment was performed using the probes described in result III-3-4. DNase I footprinting with red-OxyR revealed a clear protection pattern in the upstream regions of *ahpC*1 from -24 to -80 and from -99 to -147 (Fig. III-7A). The protected region, extending from -24 to -80, was overlapped with the -35 region of

P_{ahpC1}. DNase I footprinting was also shown the red-OxyR binding site located between +6 and -12 and between -100 and -150 in the regulatory region of *katG* (Fig. III-7B). The protected region, extending from +6 to -12, was overlapped with the -10 region of P_{katG}. Therefore these results revealed that red-OxyR presumably repressed the expression of both *ahpC*1 and *katG* by blocking RNA polymerase binding to P_{ahpC1} and P_{katG}.

III-3-7. Transcriptional regulation of *ahpC*1 and *katG* by C199S-OxyR mutant

In order to confirm whether red-OxyR repressed the expression of both *ahpC*1 and *katG*, the C199S-OxyR mutant, mimicking red-OxyR, was constructed. The C199S-OxyR mutant was produced by substituting conserved 199th cysteine of OxyR with serine. A qRT-PCR experiment was performed using the RNA isolated from wild type and C199S-OxyR mutant grown to A_{600} of 0.5 in LBS supplemented with 50 μM H_2O_2. The expression levels of *ahpC*1 and *katG* in the C199S-OxyR mutant were significantly decreased as compared to those in wild type (Fig. III-8). This result indicated that the expression of *ahpC*1 and *katG* was repressed by red-OxyR.

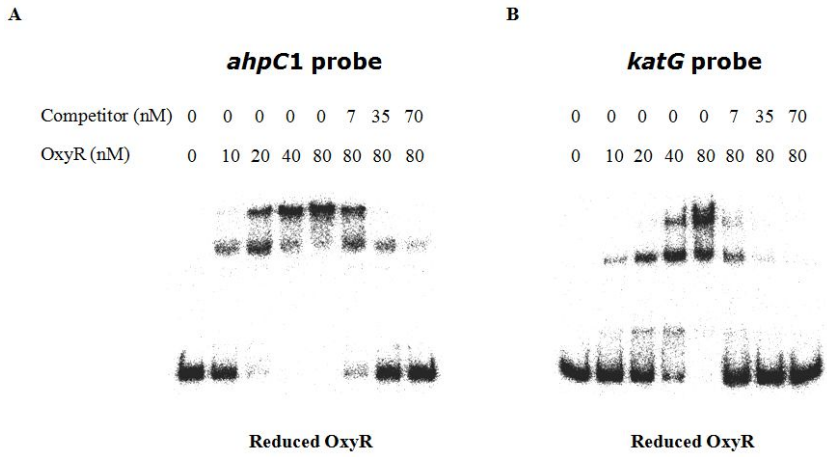

Figure III- 6. Electrophoretic mobility shift assay for reduced OxyR binding to the *ahpC*1 and *katG* regulatory regions

The EMSA reactions were performed by adding both the DNA probes used in EMSA for ox-OxyR and purified OxyR to OxyR binding buffer containing 200 mM DTT. For competition analysis, the same, but unlabeled, DNA fragments were used as competitors. Various amounts of the competitor DNAs were added to the reaction mixture as described in figure legend III-4. In lanes 6 to 8, DNA probes were incubated with OxyR and 7, 35 or 70 nM of the competitor DNA, respectively, as indicated.

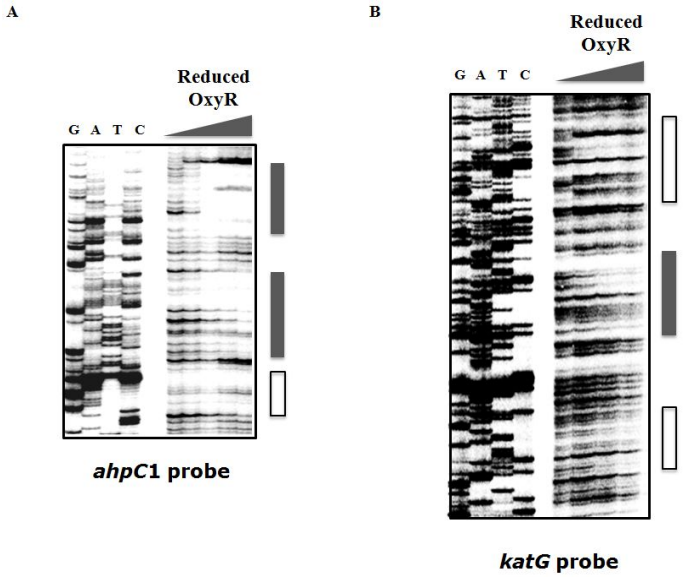

C

CTCTTCAGAAAATGGTTCCACAACGCTATCACACCAACAGTACCTATCAAAAC

ACTGCCATTAATAGGCAATACTTTTCAAATAACGCCTTTAATCCCTCAGGTAA

AATAGAAAAAGCCTATCAATAGAATAGCCACAAGCAATTTTCCTTTCGTGGGT

-35

CAGAATGTGAATATACCTCCCGAAGGCAAGCGATGCCAAACCTAACAAACTTA

-10 +1

AAGGAAATCAAGAATATGATTAACACTACTATCAAACCATTTAGCGCAACAG

RBS Start codon

D

GTTCCGCTATCTCGACAAAGTGGATGCCATCTTCTCTGACTATCCCGAACGTT

TTATCTAGCGTTCTCCCCTATCAAACCACTCGTTTTCGGATGAGTGGTTTCAA

AACATGACCTTACTGCGAACGTTTAAACAGAATTTACCTATCAAAGGAATAGA

GACAACGAATTAGATAAAACCCCACATAAGACATAGGATTAGTTTCATCAAGG

-35 -10 +1

TGCAGCGTTCGTCGTCAACTGATTCTTCGGCGTTCTGACACCTCCCTTAGAAT

AATGCGACCGACAAGGAGCAACACATGGAACACAAACCTACCCACACCAGCGG

RBS Start codon

Figure III- 7. DNase I protection analysis for identification of reduced OxyR binding site and sequence analysis of the *ahpC*1 and *katG* upstream regions

(A) The ^{32}P-labeled 410 bp *ahpC*1 regulatory region was incubated with increasing amounts of red-OxyR and then digested with DNase I. Lane 1, no OxyR added; lanes 2 to 5, red-OxyR at 100, 200, 300, and 400 nM, respectively. (B) The ^{32}P-labeled 400 bp *katG* regulatory region was incubated with increasing amounts of red-OxyR and then digested with DNase I. Lane 1, no OxyR added; lanes 2 to 6, red-OxyR at 100, 200, 300, 400, and 500 nM, respectively. Lanes G, A, T, and C represented the nucleotide sequencing ladder. The red-OxyR binding sites which was similar to ox-OxyR binding site and which was newly detected in this experiment were indicated by grey boxes and open boxes, respectively. (C, D) The transcription start site was indicated by a bent arrow. The positions of the putative -10 and -35 regions, the ATG translation initiation codon, and putative ribosomal binding sequence (RBS) were indicated in bold. The sequences proposed for the binding sites of red-OxyR were shown in dotted upper lines. The conserved nucleotide sequences for the binding of OxyR were indicated by boxes.

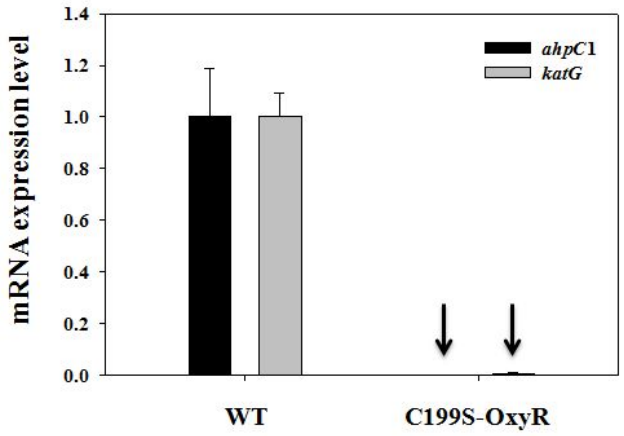

Figure III- 8. The expression levels of *ahpC*1 and *katG* in the C199S-OxyR mutant

The RNA was isolated from *V. vulnificus* wild type and C199S-OxyR mutant treated with 50 μM H_2O_2 in the exponential phase. The expression levels of *ahpC*1 and *katG* form the whole mRNA were detected.

III-4. Discussion

It has been reported that a consensus motif for the binding of ox-OxyR was defined (Michel *et al*., 1994). Although there is the consensus sequence in the P_{ahpC1} and P_{katG} of *V. vulnificus*, it has not yet been reported whether *V. vulnificus* OxyR binds experimentally to the P_{ahpC1} and P_{katG}. This study revealed that *V. vulnificus* oxidized and reduced OxyR bound to the *ahpC*1 and *katG* regulatory regions containing a specific binding site for OxyR. In addition, the specific binding site of reduced OxyR contained RNA polymerase recognition site, indicating that reduced OxyR repressed the transcriptions of both *ahpC*1 and *katG* by blocking the RNA polymerase binding to its recognition site. Interestingly, another OxyR binding site of the P_{ahpC1} between -99 and -147 was identified by the DNase I footprinting analysis. There was no OxyR binding consensus sequence in the novel OxyR binding region and no difference of the protection regions between oxidized and reduced OxyR unlike typical OxyR binding site of P_{ahpC1}. In order to determine the function of OxyR binding to the novel binding site, the Luciferase reporters, containing the P_{ahpC1} with or without the novel OxyR binding site, were constructed. Luciferase reporter assay revealed that OxyR binding to the novel binding site presumably contributed to repression of the

expression of *ahpC*1 (data not shown). In addition, another OxyR binding site of the P_{katG} between -100 and -150 was also identified by the DNase I footprinting experiment. There was no OxyR binding consensus sequence in the novel OxyR binding region of P_{katG} in the same manner. Unlike OxyR binding to the P_{ahpC1}, red-OxyR only bound to the novel binding site of P_{katG}. It was not clear what function of OxyR binding to the novel binding site was and why red-OxyR only bound to the novel binding site. Thus further study is needed to determine the accurate function of OxyR binding to the novel binding site.

Chapter IV.

Molecular analysis of promoter and intergenic region attenuator of the *Vibrio vulnificus ahpC*1*F* Operon

IV-1. Introduction

Prokaryotic genes that encode related functions are frequently organized in polycistronic operons. Such an organization is easily able to generate the coordinate expression of different cistrons of the operon. In contrast, it is difficult to express differently between the products induced by these genes within the operon. Therefore an additional step is essential for gene expression can be modulated because the cell may require the products of different genes of an operon in unequal amounts. Since each gene in a polycistronic operon is transcribed from the same promoter, different expression has to be accomplished by transcriptional termination and attenuation within the operon.

AhpF is an AhpC specific peroxiredoxin reductase that is widely distributed (Poole *et al*., 2000) and generally composes an operon with AhpC (Tartaglia *et al*., 1989; Zheng *et al*., 2001a). The *ahpCF* operon of the *Pseudomonas putida* strain gives rise to a predominant 700 bp transcript encoding *ahpC* and a less abundant 2700 bp transcript, encoding *ahpC* and *ahpF*, originating from a point 37 nucleotides upstream of the *ahpC* translation start (Fukumori and Kishii, 2001). Fukumori and Kishii discuss

that *ahpC* and *ahpCF* transcripts may result from partial read through of a terminator or processing at a stretch of sequence within the *ahpCF* intergenic region that contains several potential stem loops. Thus further work has to be done to explain this discussion. However, these studies have been still limited.

Like *Pseudomonas putida*, the organization of *ahpC*1*F* genes cluster of *V. vulnificus* is closely similar to that of *ahpCF* genes cluster of *Pseudomonas putida*. In the present study, it was revealed that *ahpC*1 and *ahpF* genes not only composed an operon but also had two transcripts even though these two genes were an operon. In addition, it was revealed that *ahpC*1 transcript was generated by attenuation at a stretch of sequence within *ahpC*1*F* intergenic region that contains a potential stem loop structure.

IV-2. Materials and Methods

IV-2-1. Strains, plasmids, and culture conditions

The strains and plasmids used in this study are listed in Table 1. *Escherichia coli* strains used for plasmid DNA replication or overexpression of protein were grown in Luria-Bertani (LB) broth or in LB broth containing 1.5% (wt/vol) agar the *V. vulnificus* strains were grown in Luria-Bertani (LB) medium supplemented with 2.0% (w/v) NaCl (LBS). All the media components were purchased from Difco (Detroit, MI), and the chemicals were purchased from Sigma (St. Louis, MO).

IV-2-2. RNA purification and northern blot analysis of the *ahpC*1*F* genes

Total cellular RNAs from *V. vulnificus* wild type, *ahpC*1 mutant, and *ahpF* mutant were isolated using a high pure RNA isolation kit (Roche, Mannheim, Germany). For Northern blot analysis, RNA was separated by agarose gel electrophoresis, transferred to nylon membrane, and hybridized as previously described. A series of reactions was performed according to standard procedures with 20 μg of total RNA for Northern blot analysis (Jeong *et al*., 2000). Two DNA probes, AHPCP and AHPFP, were labeled

with [α-^{32}P] dCTP using the prime-a-gene labeling system (Promega, Madison, WI) and used for hybridizations. The AHPCP probe was prepared by labeling the 214-bp DNA fragment, internal to *ahpC*1, amplified by PCR using primers AhpC-PR01 and AhpC-PR02 (Table 2). 228-bp DNA fragment, containing the coding region of *ahpF,* was amplified by PCR using oligonucleotide primers, AhpF-PR01 and AhpF-PR02 (Table 2) and then labeled for AHPFP probe. The blots were visualized and quantified using a phosphorimaging analyzer (model BAS1500, Fuji photo Film Co. Ltd, Tokyo, Japan) and the Image Gauge (version 3.12) program.

IV-2-3. PCR-directed linker scanning mutagenesis

PCR-directed linker scanning mutagenesis of the *ahpC*1*F* promoter region was carried out using the PCR-based on method (Gustin and Burk, 2000), with some modification. The final PCR products were subcloned into pBBRlux, a reporter containing promoterless *lux* genes, and pRK415, a broad host range vector, respectively (Fig. IV-2A). All constructions were confirmed by DNA sequencing (Macrogen, Seoul, Korea), and conjugated into the *ahpC*1 mutant of *V. vulnificus*. The cellular luminescence of the cultures was measured with a luminometer (Lumat Model 9507, Berthold, Germany) and Northern blot was performed as described in method IV-2-2.

IV-2-4. RNA ligase mediated amplification of cDNA 3'ends

The 3'RACE assay for *ahpC*1 was carried out described previously (Bensing *et al*., 1996). Briefly, total cellular RNA (3 μg) was dephosphorylated with 1 units of calf intestine alkaline phosphatase and ligated to 3'RNA adapter (5'-GCU GAU GGC GAU GAA UGA ACA CUG CUU UGA UGA AA-3') (Bioneer, Seoul, Korea). The adapter-ligated RNA was reverse-transcribed and PCR-amplified with adapter specific primer RACE-ASP and gene specific primer RACE-GSP by using a One-step RT-PCR kit (Qiagen, Valencia, CA), and then PCR product was separated by electrophoresis on 0.7% agarose gels. PCR products were then cloned into the pGEM-T Easy vector (promega, Madison, WI) and sequenced (Macrogen, Seoul, Korea).

IV-2-5. Construction of set of *ahpC*1*F* intergenic region-*lux* reporter genes transcriptional fusions

Primers, both AHPC-LR01 and AHPC-LR02 and both AHPC-LR03 and AHPC-LR04 (Table 2), were used to amplify P_{ahpC1} and 136 bp *ahpC*1*F* intergenic region, respectively. And then PCR-directed linker scanning mutagenesis used for conjunction of two DNA fragments resulted in pSS1324. The primer AHPC-LR01 was used in conjunction with one of the

following primers to amplify the DNA deletion segments of *ahpC*1*F* intergenic region: AHPC-LR05 (for pSS1325), AHPC-LR06 (for pSS1326) or AHPC-LR07 (for pSS1327) (Table 2). The 136 bp DNA fragment within *ahpC*1 ORF was amplified and ligated with P_{ahpC1} to be used as control. The DNA fragments were inserted into pBBRlux, which carries promoterless *lux* genes, to create five *lux* reporter constructs, as confirmed by DNA sequencing. The constructed *lux* reporters were then transferred into the *ahpC*1 mutant by conjugation. The cellular luminescence of the cultures was measured with a luminometer (Lumat Model 9507, Berthold, Germany).

IV-3. Results

IV-3-1. Genetic organization of the *ahpC*1*F* operon transcribed into two transcripts

The *ahpF* gene is located downstream of *ahpC*1 and the two coding regions of *ahpC*1 and *ahpF* are transcribed in the same direction (Fig. IV-1A). To investigate whether these genes were an operon, Northern blot analysis was performed using the RNA isolated from wild type, *ahpC*1 mutant, and *ahpF* mutant as described in materials and methods. It was shown that *ahpC*1*F* transcript (2.3 kb) and *ahpC*1 transcript (0.65 kb) were detected (Fig. IV-1B), that is, *ahpC*1 and *ahpF* composed an operon. Like some bacteria, there were two transcripts in the *ahpC*1*F* transcription even though these two genes were an operon. The RNA isolated from *ahpC*1 mutant did not hybridize with AHPCP probe, while the RNA derived from *ahpF* mutant was detected *ahpC*1 transcript by hybridizing with AHPCP probe. In addition, the *ahpC*1*F* transcript was only verified with AHPFP probe in wild type. However there was no transcript in the *ahpC*1 mutant (Fig. IV-1C).

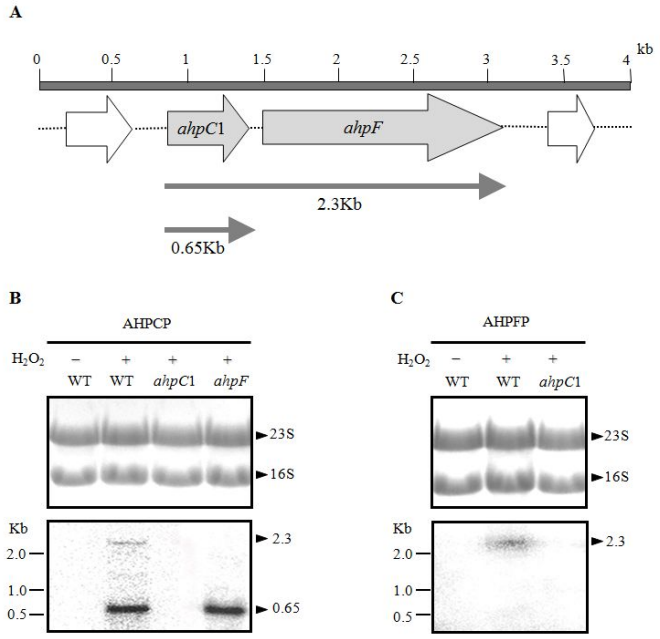

Figure IV- 1. Genetic organization of the *ahpC*1*F* operon and northern blot analysis

(A) The coding regions of *ahpC*1*F* genes (shaded arrow boxes) and chromosomal DNA (dotted lines) are shown. The direction of transcription is indicated by the arrows. (B) Total RNAs were prepared from cultures of the wild type, *ahpC*1 and *ahpF* mutants grown to exponential phase in LBS. These cultures were exposed to 250 µM hydrogen peroxide for 30 min prior to RNA extraction. The RNAs were separated (top) and hybridized to a [α-^{32}P] labelled DNA probe corresponding to the internal coding regions of *ahpC*1 (AHPCP) or *ahpF* (AHPFP) (bottom).

IV-3-2. Transcript *ahpC*1 and *ahpC*1*F* are generated by the same promoter

The 5'end for the *ahpC*1 transcripts was identified (Fig. III-1A), suggesting that *ahpC*1*F* is transcribed by one promoter, P_{ahpC1}. In order to define one promoter unambiguously, the three nucleotides of the *ahpC*1 promoter region were modified by PCR-directed linker scanning mutagenesis as indicated (Fig. IV-2A). The DNA fragments carrying these mutations were cloned into pBBRlux and pRK415 carrying *ahpC*1*F* ORF and then conjugated into *ahpC*1 mutant for luciferase assay (Fig. IV-2B) and northern blot analysis (Fig. IV-2C), respectively. The effects of the PCR-directed linker scanning mutations on *ahpC*1*F* transcription were investigated by measuring the relative luciferase unit (RLU) and detecting transcripts hybridized with AHPCP probe of each strain. In *ahpC*1 mutants carrying pSS1320, pSS1321, pSS1110 and pSS1111, the RLUs were not nearly detected and the bands corresponding to the two *ahp* transcripts were not detected in the northern blot, too. In addition, the intensities of two *ahp* transcripts in *ahpC*1 mutant carrying pSS1112 were increased with the same ratio as compared to those in *ahpC*1 mutant carrying pSS1105, respectively. Therefore these results suggested that the expression of *ahpC*1*F* was directed by a single promoter, P_{ahpC1}. Interestingly, the intensities of two *ahp*

transcripts detected in *ahpC*1 mutant carrying pSS1122 were increased as described above and the RLU of the strain with pSS1322 were higher than that with pSS1005, indicating that the mutation (G→T) in the transcription start site contributed to DNA unwinding by helicase.

IV-3-3. Determination of the 3'end of *ahpC*1 transcript by 3'RACE

To determine the 3'end of *ahpC*1 transcript, RLM-3'RACE (RNA Ligase Mediated Rapid Amplificaton of cDNA 3'ends) was performed. The cDNA synthesised was amplified and separated in agarose gel electrophoresis (Fig. IV-3A). RLM-3'RACE showed that the 3'end of *ahpC*1 transcript is located in the 83 nucleotides downstream from the translational stop codon of *ahpC*1 gene (Fig. IV-3B). When the sequence of *ahpC*1*F* intergenic region was analyzed, a large inverted repeat sequence was located in the upstream region of the 3'end of *ahpC*1 transcript (Fig. IV-3C). It suggested that there was presumably a stem loop structure in the *ahpC*1*F* intergenic region.

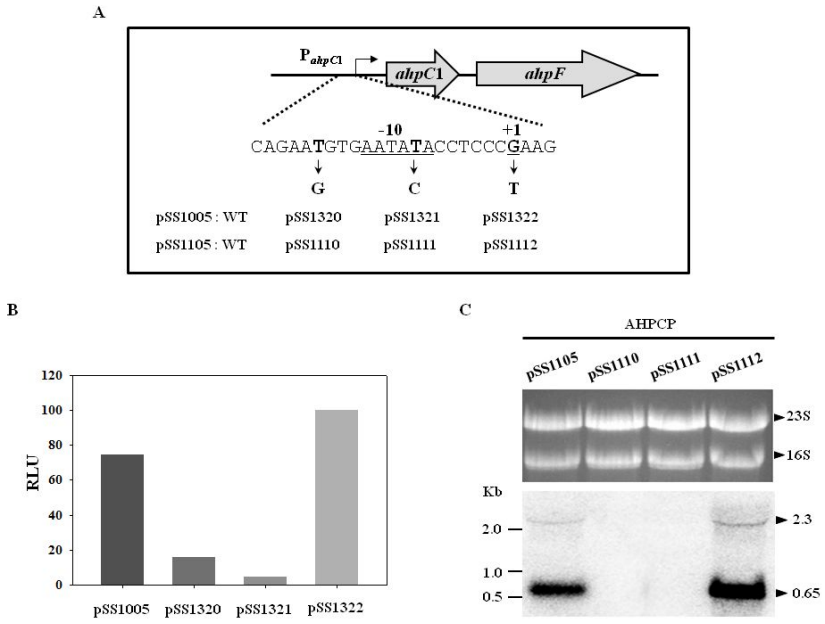

Figure IV- 2. Site directed mutagenesis and activity of *ahpC*1 promoter

(A) pSS-plasmids containing mutation introduced into the *ahpC*1 promoter were constructed. The potential -10 region is indicated by solid line. The mutations are indicated: in each case only the base designated by the arrow is replaced by a guanine residue, a cytosine residue or a thymine residue. (B) RLU were measured from cultures of the *ahpC*1 mutants containing each pSS-plasmid grown to exponential phase in LBS. (C) Total RNAs were isolated from the same condition of (B). The RNAs were separated and hybridized to [α-^{32}P] DNA probe corresponding to the internal coding regions of *ahpC*1. The expression extent of *ahp* transcript C1 and C1F is shown to the gel.

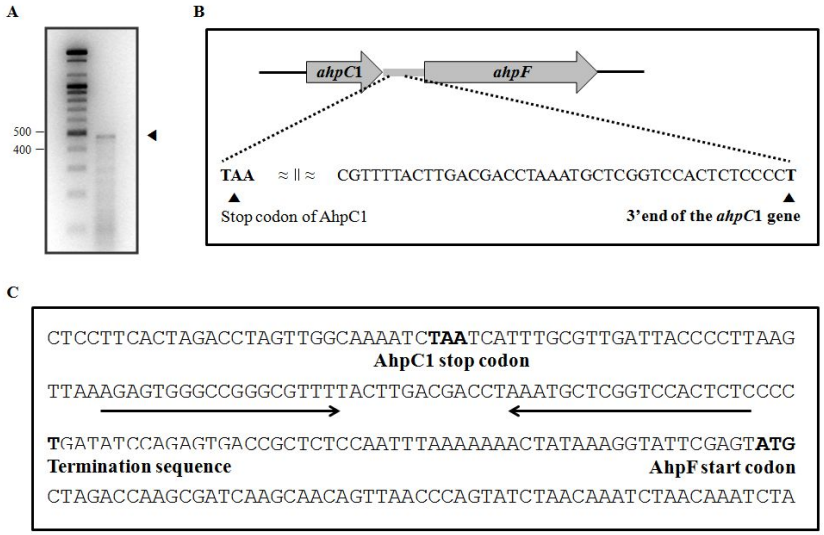

Figure IV- 3. Determination of the 3'end of *ahpC*1 transcript by 3'RACE

(A) Agarose gel electrophoresis of RLM-3'RACE products. An arrow indicates a PCR product bearing nucleotide sequences of *ahpC*1*F* intergenic region. The RLM-RACE product was cloned in a pGEMT easy vector and the nucleotide sequences were determined. (B) The coding regions of *ahpC*1*F* genes (shadow arrows) and chromosomal DNA (thick lines) are shown. The 3'end of the *ahpC*1 transcript and the stop codon (TAA) of *ahpC*1 gene are indicated by bold letters. (C) AhpC1 stop codon, AhpF start codon, and termination sequence are indicated by bold letters. Arrows indicate inverted repeat sequences in the *ahpC*1*F* intergenic region.

IV-3-4. RNA secondary structure prediction of the *ahpC*1*F* intergenic region

To explain the 3'end structure of *ahpC*1, RNA secondary structure of the *ahpC*1*F* intergenic region was predicted by using the CLC program (Fig. IV-4A). When the result was described using sequence, a stem loop structure was detected and located in the upstream region of the 3'end of *ahpC*1 transcript predicted by RLM-3'RACE (Fig. IV-4B). In addition, the stem loop structure was similar to the I-type intrinsic terminator known by Anirban *et al.* and had enough grounds for forming rho-independent transcriptional termination, that is, the 3'end stem loop structure of *ahpC*1 has stem length of 17 bases and 53 % GC contents (Fig. IV-4B). These results indicated that *ahpC*1 transcript was possibly regulated by the intrinsic terminator, stem loop structure.

IV-3-5. Transcription termination analysis of *ahpC*1*F* intergenic region

To confirm whether *ahpC*1*F* transcript could be terminated by the stem loop structure, the 136 bp and 111 bp DNA fragments including *ahpC*1*F* intergenic region were cloned into a reporter, carrying a P_{ahpC1} promoter fused to promoterless *lux* genes. The RLUs of pSS1324 and pSS1325 carrying the 136 bp and 111 bp DNA fragments, respectively, were

significantly reduced (Fig. IV-5B). However, because the insertion of random DNA fragments could reduce the RLU, 136 bp DNA fragment that did not correspond with the conditions of rho-independent terminator was selected in the functional gene of *ahpC*1 and cloned into the reporter, resulting in pSS1323. The RLU of pSS1323 was not decreased, That is, the stem loop structure located in *ahpC*1*F* intergenic region reduced the activity of promoter. In addition, the 55 bp and 30 bp DNA fragments including deleted *ahpC*1*F* intergenic region which is non-corresponding with stem-loop structure were also cloned into the reporter. The RLUs of pSS1326 and pSS1327 were much higher than those of pSS1324 and pSS1325. Collectively, it was indicated that the stem loop structure existed in *ahpC*1*F* intergenic region contributed to control the *ahpC*1 transcript.

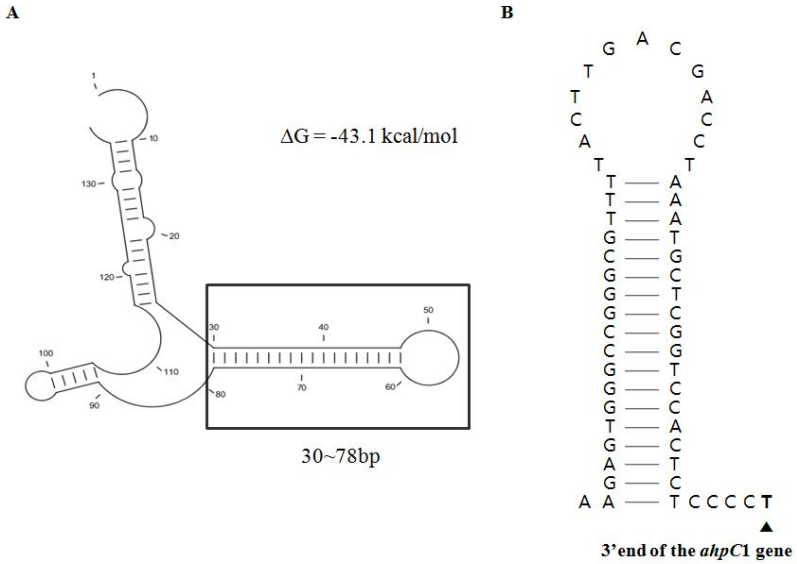

Figure IV- 4. RNA secondary structure prediction of the *ahpC*1*F* intergenic region

(A) The RNA secondary structure was predicted by RNA secondary structure prediction program (CLC program). The predicted stem-loop structure was boxed with a solid line. (B) The stem-loop structure based on (A) was described by using sequence. The 'T' sequence indicated by bold letter is the termination sequence determined by 3'RACE.

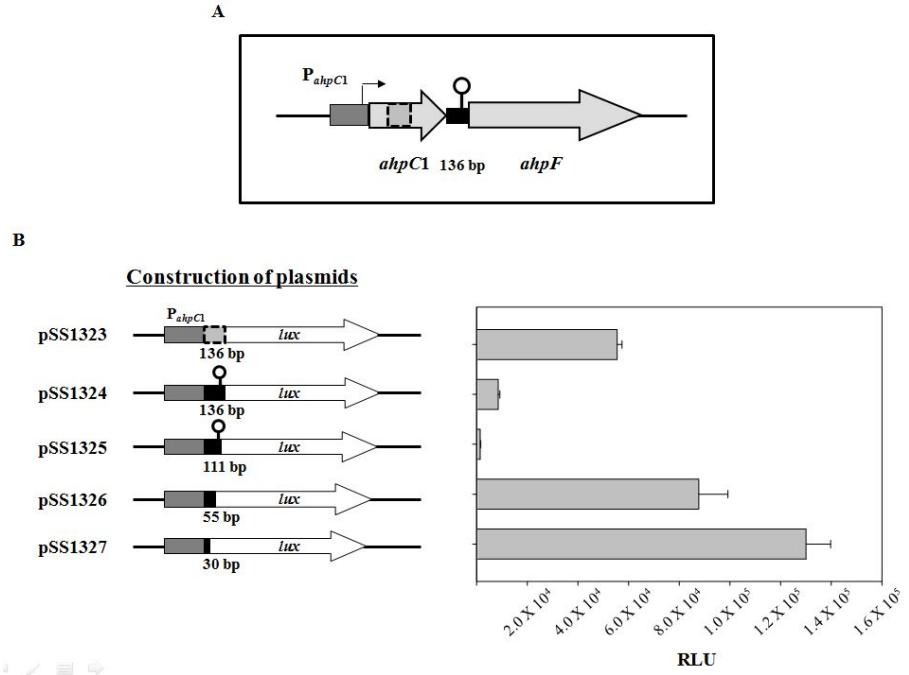

Figure IV- 5. Analysis of *ahpC*1-*ahpF* intergenic region fusions

(A) The coding regions of *ahpC*1*F* genes (arrow boxes) and chromosomal DNA (thick lines) are shown. A stem-loop structure located in the *ahpC*1*F* intergenic region indicates rho-independent transcriptional terminator of the *ahpC*1 gene and a box (dotted line) in the *ahpC*1 gene indicates 136 bp DNA fragment not having intrinsic terminators used as a positive control, pSS1323. The intergenic region of *ahpC*1*F* is indicated by a black box. (B) A reporter containing the P_{ahpC1} fused to promoterless *lux* genes was constructed. The 136 bp DNA fragment among the *ahpC*1 ORF which does not contain a termination structure and the several segments

including the different length of *ahpC*1*F* intergenic region were inserted downstream of the P_{ahpC1}. RLU were determined from the strains of *V. vulnificus* containing each plasmid as indicated.

IV-4. Discussion

Like some bacteria, *V. vulnificus ahpC*1 and *ahpF* compose an operon. Therefore it was easy to expect that *ahpC*1*F* operon produces one transcript. However, Northern blot analysis revealed that transcription of *ahpC*1*F* results in two different transcripts, *ahpC*1 transcript and *ahpC*1*F* transcript (Fig. IV-1). In order to elucidate how *ahpC*1*F* genes produce two transcripts, three hypothesizes were made. The first, *ahpC*1*F* transcripts have two promoters. The second, *ahpC*1*F* expressed from one promoter is degraded by several factors and then might result in *ahpC*1 transcript. The third, transcription of *ahpC*1*F* is regulated by rho-independent terminator to result in the *ahpC*1 transcript. Although it was proved that *ahpC*1 gene was regulated by a single promoter (Fig. III-1A), to prove the first hypothesis, mutational analysis of the regulatory region was performed and suggested that the *ahpC*1*F* operon has a single promoter (Fig. IV-2B and C). In the second place, Second theory was verified by cloning the *ahpF* isogenic mutant and Northern blot analysis (Fig. IV-1B). If the theory is correct, *ahpC*1*F* gene would not be transcribed and could not induce *ahpC*1 transcript. However, it was revealed that *ahpC*1 was still transcribed as wild type (Fig. IV-1B). Therefore, it was confirmed that *ahpC*1 is not the product

degraded from *ahpC*1*F* genes. To reveal the third hypothesis, first of all, the termination site of *ahpC*1 was determined by 3'RACE. The 3'end of *ahpC*1 transcript was located in the 83 nucleotides downstream from the stop codon of *ahpC*1 gene (Fig. IV-3B). In addition, termination was shown to occur at downstream of the stem-loop predicted by using CLC program (Fig. IV-4A and B). Generally, Rho-independent terminators consist of an inverted repeat in the primary DNA sequence, followed by a short stretch of thymine residues. However, there were the following cytosine residues of stem-loop located *ahpC*1*F* intergenic region instead of thymine residues. As it was important in controlling the expression of *ahpC*1*F* transcript via read-through as well as *ahpC*1 termination in the rho-independent terminator, it is possible to select unstable termination structure such as cytosine residues. To confirm whether transcription of *ahpC*1*F* genes can terminate by the stem-loop structures, a DNA fragment including the *ahpC*1*F* intergenic region (136 bp) was cloned into a reporter carrying a P_{ahpC1} fused to promoterless *luxCDAB*. The RLU of pSS1324 was significantly reduced (Fig. IV-5B). Interestingly, the RLU of pSS1325 was decreased than that of pSS1324. Therefore, it was predicted that *ahpC*1*F* transcript would be controlled by some factors operating in the DNA region between 111 bp and 136 bp dowmstream from the *ahpC*1 stop codon. However, because it has not yet

been established what controls *ahpC*1*F* transcript, it would be needed to identify and characterize the possible factors.

Chapter Ⅴ.

Conclusion

In the present study, Microarray detected the *Vibrio vulnificus* genes which induced under 250 μM hydrogen peroxide. A number of genes were induced and included a group of genes coding peroxiredoxin, catalase and so on. Among the genes of which expression was more induced in the cells exposed to H_2O_2, *ahpC*1 encoding an alkyl hydroperoxide reductase and *katG* encoding a catalase were selected for further characterization.

The amino acid sequence of *V. vulnificus ahpC*1 was 78% identical to those of the AhpC homologues from *E. coli* and *S. typhimurium* and their identity appeared evenly throughout the whole proteins. Phenotype of the *ahpC*1 mutant has been shown to be sensitive to various oxidants, such as H_2O_2, *t*-BOOH and CHP because AhpC1 was able to scavenge various oxidants. The system of AhpC1 as peroxiredoxin consists of AhpF as a reductant of AhpC1 and NADH as an electron donor of AhpF in *V. vulnificus*. In addition, AhpC1 is a virulence factor confirmed by infecting *in vitro* intestinal cell culture and in mice.

Unlike *E. coli*, there was only one catalase activity in *V. vulnificus*. Therefore, *V. vulnificus* KatG was responsible for the majority of the catalase activity. The phenotype of the *katG* mutant was similar to that of *ahpC*1

mutant which showed the decrease of survival under H_2O_2. However the survival of *katG* mutant under H_2O_2 was more decreased than that of *ahpC*1 mutant, indicating that *katG* is more sensitive to H_2O_2 than a*hpC*1. In contrast to the survival of *katG* mutant under H_2O_2, there was no difference in the survival between wild type and *katG* mutant under either *t*-BOOH or CHP condition. In addition, KatG is also a virulence factor confirmed by the same ways as described above.

In order to investigate the regulation of *ahpC*1 and *katG*, the promoter regions of these genes were determined by primer extension. The sequence analysis of the promoters of these two genes was revealed that there were OxyR binding consensus sequences in their regulatory regions. In addition, qRT-PCR was shown that the expression levels of *ahpC*1 and *katG* were significantly decreased in *oxyR* mutant as compared to wild type. To confirm how OxyR regulates *ahpC*1 and *katG*, EMSA was performed, indicating that OxyR was regulated the expression of *ahpC*1 and *katG* by directly binding to their promoter regions, respectively. DNase I footprinting experiment for identification of OxyR binding sequence was revealed that OxyR functioned as a class I activator activated the expression of *ahpC*1 and *katG*. It has been reported that redox sensing transcriptional regulator, OxyR, has two forms of

OxyR, Oxidized and reduced OxyR, depending on intracellular redox state. In order to verify how reduced OxyR regulates the expression of *ahpC*1 and *katG* in *V. vulnificus*, C199S-OxyR mutant, mimicking reduced OxyR, was constructed. And then the experiments described above were performed using C199S-OxyR mutant. These results indicated that reduced OxyR repressed the expression of *ahpC*1 and *katG* by physically blocking the RNA polymerase owing to OxyR binding sequence which is overlapped with RNA polymerase binding site.

Like some bacteria, in order to determine whether *V. vulnificus ahpC*1 and *ahpF* consist of an operon, Northern blot analysis was performed, indicating that *ahpC*1 and *ahpF* genes not only composed an operon but also produced two transcripts even though these two genes were regulated by a single promoter. 3'RACE was revealed 3'end of *ahpC*1 transcript and sequence analysis of *ahpC*1*F* intergenic region was shown the inverted repeat sequence located in the upstream of 3'end of *ahpC*1 transcript. Through these results, it was predicted by using CLC program that there was a stem loop structure in the *ahpC*1*F* intergenic region. In addition, it was verified that *ahpC*1 transcript was generated by attenuation at a stretch of sequence within *ahpC*1*F* intergenic region that contains a potential stem loop

structure.

On the basis of the findings from the present study, now we know that AhpC1 and KatG contribute to pathogenesis of *V. vulnificus* by enhancing the defense mechanism against oxidative stresses. In addition, new insight for controlling food-borne pathogen, *V. vulnificus*, was provided by the study for regulation of *ahpC*1 and *katG*. Especially, this study shows a possibility that *V. vulnificus* can be sufficiently controlled in food industry by using the low concentration of sanitizer which does not reduce the quality of foods.

References

Antelmann, H., and J. D. Helmann. 2011. Thiol-based redox switches and gene regulation. Antioxid. Redox Signal. **14**: 1049–1063.

Baek, W. K., H. S. Lee, M. H. Oh, M. J. Koh, K. Kim, and S. H. Choi. 2009. Identification of the *Vibrio vulnificus ahpC*1 gene and its influence on survival under oxidative stress and virulence. J. Microbiol. **47**:624-632.

Battistoni, A. *et al*. 2000. Increased expression of periplasmic Cu, An superoxide dismutase enhances survival of Eschrichia coli invasive strains within nonphagocytic cell. Infec. Immun. **68**:30-37.

Bensing, B.A., B. J. Meyer, and G. M. Dunny. 1996. Sensitive detection of bacterial transcription initiation sites and differentiation from RNA processing sites in the pheromone-induced plasmid transfer system of *Enterococcus faecalis*. Proc. Natl. Acad. Sci. **23**:7794-7799.

Bradford, M. M. 1976. A rapid and sensitive method for the quantitation of microgram quantities of protein utilizing the principle of protein-dye binding. Anal. Biochem. **72**:248-254.

Carlioz, A., and D. Touati. 1986. Isolation of superoxide dismutase mutants in *Escherichia coli*: is superoxide dismutase necessary for aerobic life? EMBO J. **5**:623-630.

Choi, H. K., N. Y. Park, D. I. Kim, H. J. Chung, S. Y. Ryu, and S. H. Choi. 2002. Promoter analysis and regulatory characteristics of *vvhBA* encoding

cytolytic hemolysin of *Vibrio vulnificus*. J. Biol. Chem. **277**:47292-47299.

Christman, M. F., R.W. Morgan, F. S. Jacobson, and B. N. Ames. 1985. Positive control of a regulon for defences against oxidative stress and some heat-shock proteins in *Salmonella typhimurium*. Cell. **41**:753-762.

Christman M. F., G. Storz, B. M. Ames. 1989. OxyR, a positive regulator of hydrogen peroxide-inducible genes in *Escherichia coli* and *Salmonella typhimurium*, is homologous to a family of bacterial regulatory proteins. Proc. Natl. Acad. Sci. **86**: 3484–3488.

Falkow, S. 1988. Molecular Koch's postulates applied to microbial pathogenicity. Rev. Infect. Dis. **10**:274-276.

Fang, F. C. *et al.* 1999. Virulent *Salmonella typhimurium* has two periplasmic Cu, Zn-superoxide dismutases. Proc. Natl. Acad. Sci. USA. **13**:7502-7507.

Feldhusen, F. 2000. The role of seafood in bacterial foodborne diseases. Microbes Infect. **2**:1651-1660.

Fukumori, F., and M. Kishii. 2001. Molecular cloning and transcriptional analysis of the alkyl hydroperoxide reductase genes from *Pseudomonas putida* KT2442. J. Gen. Appl. Microbiol. **47**:269-277.

Goo, S. Y. *et al.* 2006. Identification of OmpU of *Vibrio vulnificus* as a fibronectin-binding protein and its role in bacterial pathogenesis. Infect. Immun. **74**:5586–5594.

Greenberg, J. T., and B. Demple. 1988. Overproduction of peroxide-scavenging enzymes in *Escherichia coli* suppresses spontaneous mutagenesis and

sensitivity to redox-cycling agents in *oxyR* mutants. EMBO J. **7**:2611-2617.

Gustin, K., and R. D. Burk. 2000. PCR-Directed Linker Scanning Mutagenesis. Methods. Mol. Biol. **130**:85-90.

Hoi, L., J. L. Larsen, I. Dalsgaard, and A. Dalsgaard. 1998. Occurrence of *Vibrio vulnificus* biotypes in Danish marine environments. Appl. Environ. Microbiol. **64**:7-13.

Jacobson, F. S., R. W. Morgan, M. F. Christman, and B. M. Ames. 1989 An alkyl hydroperoxide reductase induced by oxidative stress in *Salmonella typhimurium* and *Escherichia coli*: genetic characterization and cloning of *ahp*. J. Bacteriol. **171**:2049-2055.

Janssen, R., T. Straaten, A. Diepen, and J. T. Dissel. 2003. Responses to reactive oxygen intermediates and virulence of salmonella typhimuriu. Microbes. Infec. **5**:527-534

Jeong, W., M. K. Cha, and I. H. Kim. 2000. Thioredoxin-dependent hydroperoxide peroxidase activity of bacterioferritin comigratory protein (BCP) as a new member of the thiol-specific antioxidant protein (TSA)/alkyl hydroperoxide peroxidase C (AhpC) family. J. Biol. Chem. **275**:2924-2930.

Jeong, H. G., and S. H. Choi. 2008 Evidence that AphB essential for the virulence of *Vibrio vulnificus* is a global regulator. J. Bacteriol. **190**:3768-3773.

Jones, M. K., and J. D. Oliver. 2009. *Vibrio vulnificus*: Disease and Pathogenesis. *Infect. Immun.* (Epub ahead of print)

Jönsson, T. J., H. R. Ellis, and L. B. Poole. 2007. Cysteine reactivity and thiol-

disulfide interchange pathways in AhpF and AhpC of the bacterial alkyl hydroperoxide reductase system. Biochemistry. **46**:5709-5721

Kang, I. H., J. S. Kim, and J. K. Lee. 2007. The virulence of *Vibrio vulnificus* is affected by the cellular level of superoxide dismutase activity. J. Microbiol. Biotechnol.**17**:1399-1402.

Kim, H. S., S. J. Park, and K. H. Lee. 2009. Role of NtrC-regulated exopolysaccharides in the biofilm formation and pathogenic interaction of *Vibrio vulnificus*. Mol. Microbiol. **74:**436–453.

Lee, J. H., M. W. Kim, B. S. Kim, S. M. Kim, B. C. Lee, T. S. Kim, and S. H. Choi. 2007. Identification and characterization of the *Vibrio vulnificus rtxA* essential for cytotoxicity in vitro and virulence in mice. J. Microbiol. **45**:146-152.

Lenz, D. H., K.C. Mok, B. N. Lilley, R. V. Kulkarni, N. S. Wingreen, and B. L. Bassler. 2004. The small RNA chaperone Hfq and multiple small RNAs control quorum sensing in *Vibrio harveyi* and *Vibrio cholera*. Cell. **118**:69-82.

Linkous, D. A., and J. D. Oliver. 1999. Pathogenesis of *Vibrio vulnificus*. FEMS Microbiol. Lett. **174**:207-214.

Mead PS, S. L. *et al*. 1999. Food-related illness and death in the United States. Emerg. Infect. Dis. **5**:607-625.

Mekalanos, J. J. 1992. Environmental signals controlling expression of virulence determinants in bacteria. J. Bacteriol. **174**:1-7.

Merkel, S. M., S. Alexander, E. Zurall, J. D. Oliver, and Y. M. Huet-Hudson.

2001. Essential role for estrogen in protection against *Vibrio vulnificus* induced endotoxic shock. Infect. Immun. **69**:6119-6122.

Michel, B. *et al.* 1994. Redox-Dependent Shift of OxyR-DNA Contacts along an Extended DNA-Binding Site: A Mechanism for Differential Promoter Selection. Cell. **78**:897-909.

Miller, R. A. and B. E. Britigan. 1997. Role of oxidants in microbial pathophysiology. Clinical Microbiology Reviews. **10**:1-18.

Miller, V. L. and J. J. Mekalanos. 1988. A novel suicide vector and its use in construction of insertion mutations: osmoregulation of outer membrane proteins and virulence determinants in *Vibrio cholerae* requires *toxR*. J. Bacteriol. **170**:2575-2583.

Milton, D. L., R. O'Toole, P. Horstedt, and H. Wolf-Watz. 1996. Flagellin A is essential for the virulence of *Vibrio anguillarum*. J. Bacteriol. **178**:1310-1319.

Mishra, S., and J. Imlay. 2012. Why do bacteria use so many enzymes to scavenge hydrogen peroxide?. Archiv. Biochem. Biophys. **525**:145-160

Morikawa, K. *et al.* 2006. Bacterial nucleoid dynamics: oxidative stress response in *Staphylococcus aureus*. Genes Cells **11**: 409–423.

Mulvey, M. R., J. Switala, A. Borys, and P. C. Loewen. 1990. Regulation of transcription of *katE* and *katF* in *Escherichia coli*. J. Bacteriol. **172**:6713-6720.

Myatt, D. C., and G. H. Davis. 1989 Isolation of medically significant *Vibrio* species from riverine sources in the south east Queensland. Microbios. **60**:111-123.

Neidhardt F. C., A. S. Lynch, and C. C. Lin E. 1996. In E. coli and Salmonella: Cellular and Molecular Biology VI, ed Neidhardt F. C. (American Society for Microbiology Press, Washington, D. C.) 2nd Ed. pp 1526–1538.

Oh, M. H., S. M. Lee, D. H. Lee, and S. H. Choi. 2009. Regulation of the *Vibrio vulnificus hupA* gene by temperature alteration and cyclic AMP receptor protein and evaluation of its role in virulence. Infect. Immun. **77**:1208-1215.

Oka, A., H. Sugisaki, and M. Takanami. 1981. Nucleotide sequence of the kanam ycin resistance transposon Tn903. J. Mol. Biol. **147**:217-226.

Park, K. J., M. J. Kang, S. H. Kim, H. J. Lee, J. K. Lim, S. H. Choi, S. J. Park, and K. H. Lee. 2004. Isolation and characterization of *rpoS* in a pathogenic bacterium, *Vibrio vulnificus*: Role of σ^S in survival of exponential phase cells under oxidative stress. J. Bacteriol. **186**:3304-3312.

Park, N. Y., J. H. Lee, M. W. Kim, H. G. Jeong, B. C. Lee, T. S. Kim, and S. H. Choi. 2006. Identificatioin of *Vibrio vulnificus wbpP* gene and evaluation of its role in virulence. Infect. Immun. **74**:721-728.

Park, J. H., Y. Cho, J. Chun, Y. Seok, J. K. Lee, K. S. Kim, K. Lee, S. Park and S. H. Choi. 2011. Complete genome sequence of *Vibrio vulnificus* MO6-24/O. J. Bacteriol. **193**:2062.

Poole *et al.* 2000. *Streptococcus mutans* H_2O_2-forming NADH oxidase is an alkyl hydroperoxide reductase protein**.** J. Free. Radi. Biol. Med. **28**:108–120.

Poole, L. B. 2003. Bacterial Peroxiredoxins, p. 81-101. *In* H.J. Forman, J.M.

Fukuto and M. Torres, Signal Transduction by Reactive Oxygen and Nitrogen Species: Pathways and Chemical Principles.

Poole, L. B. 2005. Bacterial defenses against oxidants: mechanistic features of cysteine-based peroxidases and their flavoprotein reductases. Arch. Biochem. Biophys. **433**:240–254.

Reed, L. J. and H. Muench. 1938. A simple method of estimating fifty percent endpoints. Am. J. Hyg. **27**:439-497.

Sambrook, J., E. F. Fritsch, and T. Maniatis. 1989 Molecular Cloning: A Laboratory Manual, 2nd Ed.**,** Cold Spring Harbor Laboratory, Cold Spring Harbor, NY

Schell, M. A. 1993. Molecular biology of the LysR family of transcriptional regulators. Annu. Rev. Microbiol. **47**: 597–626.

Seaver, L. C., and J. A. Imlay. 2001a. Alkyl Hydroperoxide Reductase Is the Primary Scavenger of Endogenous Hydrogen Peroxide in Escherichia coli. J. Bac. **183**:7173-7181

Seaver, L. C., and J. A. Imlay. 2001b. Hydrogen peroxide fluxes and compartmentalization inside growing *Escherichia coli*. J. Bacteriol. **183**: 7182–7189.

Storz, G., and J. A. Imlay. 1999. Oxidative stress. Curr. Opin. Microbiol. **2**:188–194.

Storz, G., and M. Zheng. 2000. Oxidative stress, p. 47–59. *In* G. Storz and R. Hennge-Aronis, Bacterial stress responses. American Society for Microbiology,

Washington, D.C., USA.

Strom, M. and R.N. Paranjpye. 2000. Epidemiology and pathogenesis of *Vibrio vulnificus*. Microbes. Infect. **2**:177-188.

Tartaglia, L. A., G. Storz, and B. M. Ames. 1989. Identification and molecular analysis of *oxyR*-regulated promoters important for the bacterial adaptation to oxidative stress. J. Mol. Biol. **210**:709-719.

Toledano, M. B. *et al.* 1994. Redox-dependent shift of OxyR-DNA contacts along an extended DNA-binding site: a mechanism for differential promoter selection. Cell **78**: 897–909.

Wang, G., A. A. Olczak, J. P. Walton, and R. J. Maier. 2005. Contribution of the *Helicobacter pylori* thiol peroxidase bacterioferritin comigratory protein to oxidative stress resistance and host colonization. Infect. Immun. **73**:378-384.

Wood, M. J., E. C. Andrade, and G. Storz. 2003. The redox domain of the Yap1p transcription factor contains two disulfide bonds. Biochem. **42**:11982-11991.

Zheng, M., B. Doan, T. D. Schneder, G. Storz. 1999. OxyR and SoxRS regulation of *fur*. J. Bacteriol. **181**: 4639–4643.

Zheng, M., X. Wang, B. Doan, K.A. Lewis, T.D. Schneider, and G. Storz. 2001a. Computation-directed identification of OxyR DNA binding sites in *Escherichia.* J. Bacteriol. **185**:4571-4579.

Zheng, M. *et al.* 2001b. DNA microarray-mediated transcriptional profiling of the *Escherichia coli* response to hydrogen peroxide. J. Bacteriol. **183**: 4562–4570.

국문초록

패혈증 비브리오 균은 어패류의 생식이나 상처부위를 통하여 인체를 감염시켜 높은 치사율의 패혈증을 유발하는 병원성 미생물이다. 이러한 병원성 미생물은 감염되었을 때, 숙주의 급격한 환경 변화를 극복하고 병원성을 유발하기 위한 과정이 필요하다. 특히 숙주세포의 주요 방어 기제의 하나인 산화적 스트레스를 극복하고 생존하기 위해 병원균은 정교한 메커니즘을 진화시켜 왔다. 또한 식품산업에서 병원성 미생물을 제어하기 위해 살균 과정 중 하나의 방법으로 산화적 스트레스를 이용하고 있다. 그러나 식품의 품질 저하 우려 때문에 그 사용 농도가 제한되어 있어 병원균이 진화시켜온 정교한 메커니즘으로 산화적 스트레스를 극복하여 살균 과정에서 생존할 가능성이 존재한다. 따라서 본 연구는 산화적 스트레스를 극복하기 위해 유도되는 유전자를 찾고, 이 유전자의 기능과 조절 기작을 분석하여 패혈증 비브리오 균의 병원성을 조절할 수 있는 이론적 근거를 마련하기 위해 진행하였다.

산화적 스트레스를 받지 않은 균과 받은 균을 비교하는 microarray 실험에서 *ahpC*1과 *katG* 유전자들이 선택되었고, 그들의 기능을 확인하기 위해 두 유전자를 각각 불화성화 시켜 돌연변이 균주를 만들었다. 배지에 과산화수소를 첨가하여 산화적 스트레스를 유도하고 정상 균주와 돌연변이 균주를 비교하였을 때, 두 돌연변이 균주 모두 성장이 저해되는 것을 확인할 수 있었다.

그러나 유기 과산화물을 첨가하여 산화적 스트레스를 유도하였을 때, *ahpC*1 돌연변이 균주는 과산화수소를 처리한 경우와 마찬가지로 성장이 저해되는 것을 확인 할 수 있었지만, *katG* 돌연변이 균주는 정상 균주와 성장에서 큰 차이를 보이지 않았다. 이 두 유전자들이 항산화 기능이 있는지 확인하기 위해 효소 활성 실험과 catalase 활성을 측정하는 실험을 각각 진행하였을 때, AhpC1은 AhpF, NADH와 같이 존재할 때 가장 높은 항산화 능력을 보였고 KatG는 항산화 능력인 catalase 활성이 있음을 확인 할 수 있었다. *ahpC*1과 *katG* 유전자가 비브리오 패혈증 균의 세포 독성을 줄이는 효과가 있는지 확인하기 위해 장내 상피 세포인 INT-407을 이용하여 세포 독성을 측정하여 보았다. 그 결과 두 돌연변이 균주는 정상 균주에 비해 낮은 세포 독성을 나타내는 것을 확인하였고, 실제 *in vivo* 모델인 mice 실험에서 역시 정상 균주를 감염시켰을 경우보다 돌연변이 균주를 감염시켰을 경우, mice의 생존률이 더 높은 것을 확인하였다. 따라서 AhpC1과 KatG는 항산화 효소의 역할을 하고 숙주세포에 감염되었을 때 산화적 스트레스를 극복하게 하여 비브리오 패혈증 균이 병원성을 유지할 수 있도록 한다.

AhpC1과 KatG의 조절 기작을 확인하기 위해 프로모터를 찾고 프로모터의 시퀀스를 분석을 하였다. 두 유전자에서 모두 OxyR 조절자의 공통배열이 존재하였고, EMSA와 DNase I footprinting 실험을 통해 OxyR은 산화된 OxyR과 환원된 OxyR이 모두 *ahpC*1과 *katG*의 프로모터에 직접 붙어서 그 둘의

발현을 조절하는 것을 확인하였다. OxyR이 붙는 시퀀스를 분석하고 qRT-PCR을 이용하여 산화된 OxyR은 두 유전자를 활성화 시키고, 반면 환원된 OxyR은 그것의 붙는 위치가 RNA 중합효소가 두 유전자의 프로모터에 붙는 위치와 겹치게 되어 두 유전자의 발현을 감소시킨다는 것을 확인하였다.

앞에서 AhpC1은 AhpF와 함께 역할을 할 때, 항산화 효소의 역할이 극대화 되는 것을 확인하였다. 유전자 집단을 분석한 결과를 통해 두 유전자는 오페론으로 발현할 것으로 예측되었고, northern blot 실험을 통해 두 유전자가 오페론임을 확인하였다. 실험 결과에서 오페론으로 확인되는 전사 band 이외에 *ahpC*1 유전자의 크기와 비슷한 전사 band가 존재하는 것을 발견하였다. 전사 band가 두 개이기 때문에 *ahpC*1*F* 오페론이 두개의 프로모터에 의해 조절되는지 가정하였고, 실험 결과 하나의 프로모터에 의해서 조절 받는다는 것을 알 수 있었다. *ahpC*1 유전자와 *ahpF* 유전자 사이의 non-coding 지역 (intergenic region)에서 전사의 감쇄가 일어날 가능성을 두고 먼저 정확한 감쇄 위치를 확인하였다. 또한 이 intergenic region의 RNA 2차 구조를 예측하였을 때, stem-loop 구조를 확인할 수 있었고 앞에서 밝힌 감쇄 위치 바로 앞에 위치하는 것으로 보아 stem-loop 구조가 감쇄에 역할을 할 것으로 예측되었다. 다양한 길이의 intergenic region 의 DNA 조각들을 이용하여 리포터 시스템을 구축하였고, 그 결과 intergenic region에 존재하는 stem-loop 구조가 *ahpC*1*F*의 전사 감쇄를 유도한다는 것을 확인하였다.

이 연구는 앞에서 밝힌 *ahpC*1과 *katG*의 기능적 특성을 통해 항산화 측면에서 비브리오 패혈증 균의 병원성에 두 유전자가 관여하고 있다는 것을 알 수 있었고, 조절 기작에 대한 연구를 통해 비브리오 패혈증 균의 제어에 대한 새로운 가능성을 제시하여 주었다. 특히 식품 산업에서 식품의 품질을 저해하지 않는 낮은 농도의 산화적 스트레스를 이용하여 충분히 비브리오 패혈증 균을 제어할 수 있는 가능성을 제시하였다.

주요어 : 패혈증 비브리오균, AhpC1, KatG, 산화적 스트레스, OxyR, AhpF

학 번 : 2007-23171